

## ■ Porphyrin Aggregates

Porphyrin/Platinum(II) C<sup>^</sup>N<sup>^</sup>N Acetylide Complexes: Synthesis, Photophysical Properties, and Singlet Oxygen GenerationAtanu Jana,<sup>\*,[a]</sup> Luke McKenzie,<sup>[a]</sup> Ashley B. Wragg,<sup>[a]</sup> Masatoshi Ishida,<sup>[b]</sup> Jonathan P. Hill,<sup>[c]</sup> Julia A. Weinstein,<sup>[a]</sup> Elizabeth Baggaley,<sup>[a]</sup> and Michael D. Ward<sup>\*,[a]</sup>*Dedicated to Professor Jonathan L. Sessler on the occasion of his 60th birthday*

**Abstract:** A new class of substituted porphyrins has been developed in which a different number of cyclometalated Pt<sup>II</sup> C<sup>^</sup>N<sup>^</sup>N acetylides and polyethylene glycol (PEG) chains are attached to the *meso* positions of the porphyrin core, which are meant for photophysical, electrochemical, and in vitro light-induced singlet oxygen (<sup>1</sup>O<sub>2</sub>) generation studies. All of these Zn<sup>II</sup> porphyrin–Pt<sup>II</sup> C<sup>^</sup>N<sup>^</sup>N acetylide conjugates show moderate to high ( $\Phi_{\Delta}$  = 0.55 to 0.63) singlet oxygen generation efficiency. The complexes are soluble in organic solvents but, despite the PEG substituents, slowly aggregate

in aqueous solvent systems. These conjugates also exhibit interesting photophysical properties, including near-complete photoinduced energy transfer (PEnT) through the rigid acetylenic bond(s) from the Pt<sup>II</sup> C<sup>^</sup>N<sup>^</sup>N antenna units to the Zn<sup>II</sup> porphyrin core, which shows sensitized luminescence, as shown by quenching of Pt<sup>II</sup> C<sup>^</sup>N<sup>^</sup>N-based luminescence. Electrochemical measurements show a set of redox processes that are approximately the sum of what is observed for the Pt<sup>II</sup> C<sup>^</sup>N<sup>^</sup>N acetylide and Zn<sup>II</sup> porphyrin units. UV/Vis spectroscopic properties are supported by DFT calculations.

## Introduction

Porphyrins are interesting because of their unique photophysical and electrochemical properties<sup>[1]</sup> as well as their wide range of applications. They are extensively used in various research areas as diverse as three dimensional optical data-storage,<sup>[2]</sup> dye-sensitized solar cells,<sup>[3]</sup> photodynamic therapy (PDT),<sup>[4]</sup> multiphoton imaging,<sup>[5]</sup> and photogeneration of <sup>1</sup>O<sub>2</sub> for a range of biological applications,<sup>[6]</sup> and sensing.<sup>[7]</sup> Furthermore, their photophysical properties make them desirable components to be incorporated in multinuclear assemblies in which they are covalently attached to energy- or electron-donors (or acceptors)

for applications such as generating charge-separated excited states and artificial molecular electronic devices.<sup>[8]</sup>

There are a number of Pt<sup>II</sup> N<sup>^</sup>N<sup>^</sup>N,<sup>[9]</sup> Pt<sup>II</sup> N<sup>^</sup>C<sup>^</sup>N,<sup>[10]</sup> Pt<sup>II</sup> C<sup>^</sup>N<sup>^</sup>C,<sup>[11]</sup> and Pt<sup>II</sup> C<sup>^</sup>N<sup>^</sup>N<sup>[12]</sup>-types of organoplatinum lumino-phoric materials reported to date. These compounds exhibit interesting photophysical behavior and are promising candidates for cellular imaging studies<sup>[10b,12d–e]</sup> and photovoltaic applications.<sup>[10d,12b]</sup> However, relatively little attention has been paid<sup>[13]</sup> to the attachment of such cyclometalated chromophoric units to the periphery of a porphyrin core for making hybrid supra-molecular systems, with the two different photoactive moieties being fused together in a single skeleton by rigid conjugation. It is expected that hybrid supramolecular systems of this nature could show interesting photophysical behavior for a range of applications, and the cyclometallated Pt<sup>II</sup> units from this family are well known for their outstanding photophysical properties and the applications which arise from them.<sup>[10–12]</sup>

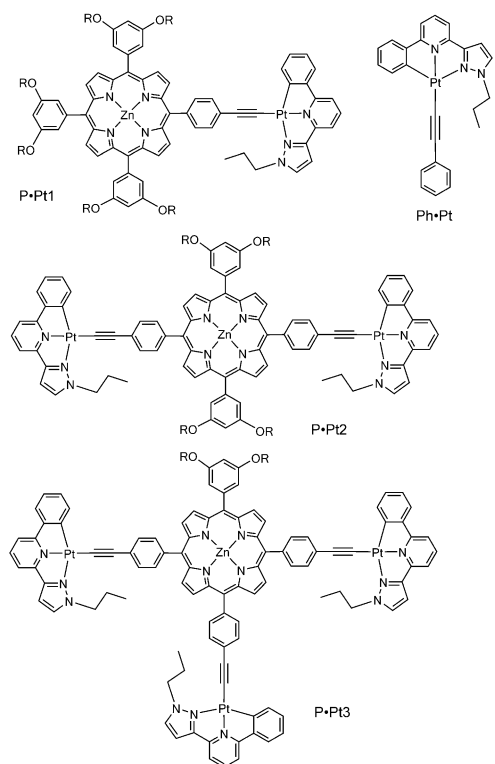
Herein, we report the synthesis of a series of porphyrins (Scheme 1) in which different numbers of Pt<sup>II</sup> C<sup>^</sup>N<sup>^</sup>N acetylide units and PEG chains are appended to the *meso* positions of the porphyrin core. These combine two types of photoactive unit (the Pt<sup>II</sup> C<sup>^</sup>N<sup>^</sup>N unit and the Zn<sup>II</sup> porphyrin unit) in a single covalently linked assembly. With a view to possible biological applications (luminescence imaging, PDT) they have been partly water-solubilized by incorporation of hydrophilic PEG chains onto the *meso* phenyl substituents. We have also synthesized a mononuclear Pt<sup>II</sup> C<sup>^</sup>N<sup>^</sup>N complex as a reference compound for photophysical and electrochemical studies. The compounds show a range of interesting properties including effective <sup>1</sup>O<sub>2</sub> generation, photoinduced energy transfer from

[a] Dr. A. Jana, L. McKenzie, Dr. A. B. Wragg, Prof. J. A. Weinstein, Dr. E. Baggaley, Prof. Dr. M. D. Ward  
Department of Chemistry, University of Sheffield  
Sheffield, S3 7HF (United Kingdom)  
E-mail: atanuj78@gmail.com  
m.d.ward@sheffield.ac.uk

[b] Dr. M. Ishida  
Education Center for Global Leaders in Molecular Systems for Devices,  
Kyushu University Fukuoka 819-0395 (Japan)

[c] Dr. J. P. Hill  
World Premier International (WPI) Research Center for Materials Nanoarchitectonics (MANA), National Institute for Materials Science (NIMS)  
Namiki (Tsukuba) Ibaraki 305-0044 (Japan)

Supporting information for this article (detailed experimental procedures including the SEM synthetic procedures, NMR spectra for all the compounds and references, selected bond lengths and angles for reference complex P-Pt, additional figures for electrochemical experiments, results from DFT calculations, TD-DFT analysis) is available on the WWW under <http://dx.doi.org/10.1002/chem.201504509>.



**Scheme 1.** Structure of the Pt<sup>II</sup>C<sup>N</sup>N-acetylide appended Zn<sup>II</sup> porphyrin complexes, with the reference compound **Ph+Pt** used in the present study. R = (CH<sub>2</sub>CH<sub>2</sub>O)<sub>3</sub>Me.

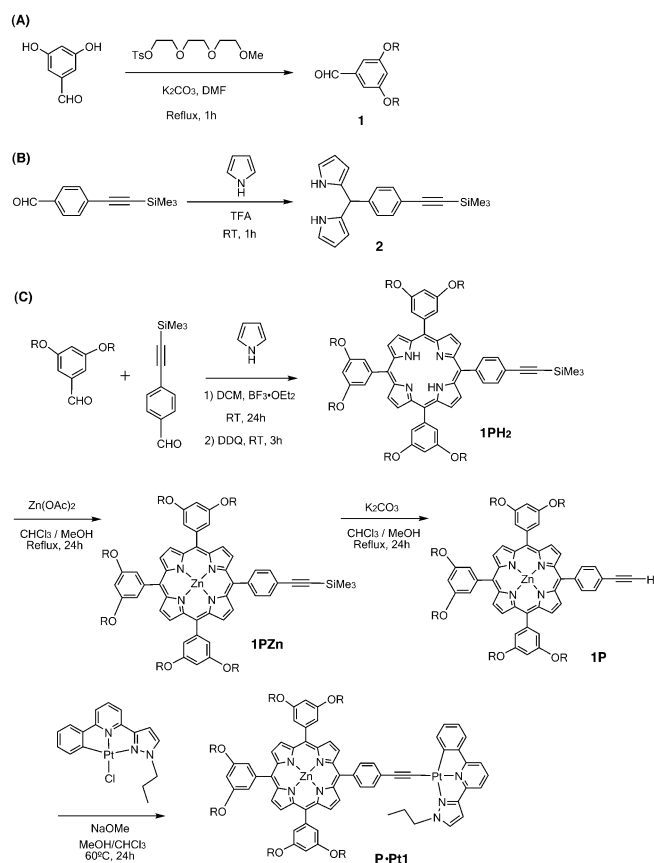
the Pt<sup>II</sup> units to the Zn<sup>II</sup> porphyrin core, and solvent-dependent aggregation. The photophysical properties discussed herein are supported by the theoretical calculations.

## Results and Discussion

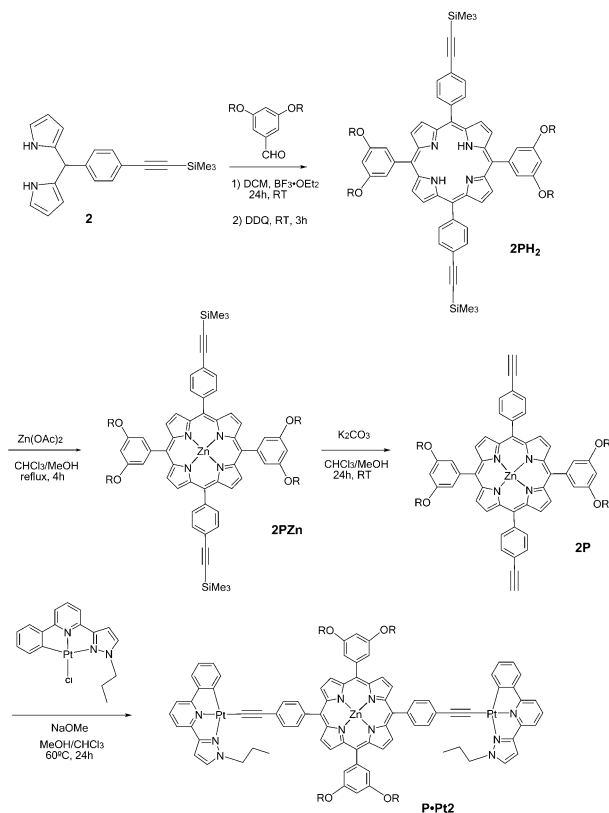
### Synthesis and characterization

All of the porphyrin precursors, namely **1PH2** (Scheme 2), **2PH2** (Scheme 3), and **3PH2** (Scheme 4), bearing pendant alkyne groups protected with TMS units, were synthesized by the conventional acid catalyzed (BF<sub>3</sub>·OEt<sub>2</sub>) pyrrole-aldehyde macrocyclization reaction (Lindsay's technique) in CH<sub>2</sub>Cl<sub>2</sub>, followed by oxidation with 2,3-dichloro-5,6-dicyano-1,4-benzoquinone (DDQ).<sup>[14]</sup> Upon varying the ratio of the aldehyde mixture of PEG-ylated benzaldehyde **1** and TMS-alkynyl benzaldehyde, the mono-TMS-alkynyl derivative **1PH2** and tris(TMS-alkynyl) derivative **3PH2** were predominantly obtained (Scheme 2 and Scheme 4, respectively). The di-substituted derivative, **2PH2** was prepared by [2+2]-MacDonald condensation of dipyrromethane **2** and aldehyde **1** (Scheme 3).

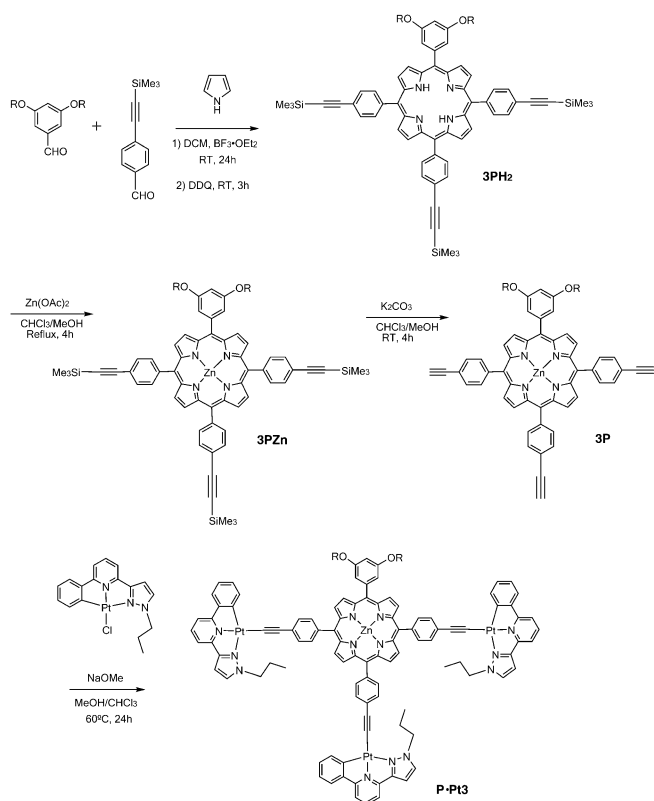
The obtained porphyrins were purified by several rounds of column chromatography on Al<sub>2</sub>O<sub>3</sub> and SiO<sub>2</sub>. The Zn<sup>II</sup> complexes of each isolated porphyrin, that is, **nPZn** (*n* = 1–3), were obtained by reaction with anhydrous Zn(OAc)<sub>2</sub> in CHCl<sub>3</sub>/MeOH (10:1) under reflux. The porphyrin–platinum linked products, **P+Ptn**, (where *n* = 1–3) were synthesized by removal of the TMS protecting groups of **nP** (*n* = 1–3) with K<sub>2</sub>CO<sub>3</sub> to generate the



**Scheme 2.** Preparation of precursors **1** and **2**, and of **P+Pt1**. R = (CH<sub>2</sub>CH<sub>2</sub>O)<sub>3</sub>Me.



**Scheme 3.** Preparation of **P+Pt2**. R = (CH<sub>2</sub>CH<sub>2</sub>O)<sub>3</sub>Me.



**Scheme 4.** Preparation of P-Pt3. R = (CH<sub>2</sub>CH<sub>2</sub>O)<sub>3</sub>Me.

terminal alkynes; this was followed by coupling with previously-prepared organoplatinum complex, Pt<sup>II</sup> C<sup>^</sup>N<sup>^</sup>N<sup>^</sup>Cl in the presence of NaOMe, as reported by Williams and co-workers.<sup>[10c]</sup> The final products were all purified by using a Sephadex column to remove excess Pt<sup>II</sup> C<sup>^</sup>N<sup>^</sup>N<sup>^</sup>Cl and obtain the materials in pure form. The result is a series of complexes in which one, two, or three Pt<sup>II</sup> C<sup>^</sup>N<sup>^</sup>N<sup>^</sup> units are connected to the Zn<sup>II</sup> porphyrin core by ethynylphenyl linkages to the *meso* positions, and three, two, or one aromatic groups are attached at the remaining positions. NMR and mass spectroscopic analysis support the proposed structures.

We also prepared the phenyl-substituted platinum complex Ph-Pt, by reaction of Pt<sup>II</sup> C<sup>^</sup>N<sup>^</sup>N<sup>^</sup>Cl with phenylacetylene, as a reference for photophysical studies. The crystals of Ph-Pt suitable for X-ray crystallographic analysis were obtained from CHCl<sub>3</sub>/hexane. The molecular structure of Ph-Pt shows the expected four-coordinate square-planar Pt<sup>II</sup> coordination geometry in which the phenyl group of the alkyne substituent is nearly perpendicular to the Pt<sup>II</sup> C<sup>^</sup>N<sup>^</sup>N<sup>^</sup> mean plane (Figure 1). Selected bond lengths and angles are given in Table 1. The structure reveals the presence of two crystallographically independent complex molecules in the asymmetric unit (Figure 1b) with the shortest Pt1...Pt2 separation of 9.890 Å, indicating no metal-metal interaction in solid state.

### Absorption spectra and solution aggregation

UV/Vis absorption spectra of all the compounds were carried out in MeCN, and also in water/DMSO (97:3). The absorption

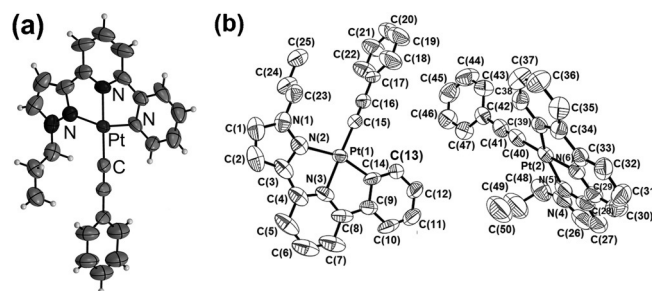


**Figure 1.** a) The molecular structure of Ph-Pt from single crystal data; b) the two independent complexes in the asymmetric unit. Ellipsoids are set at 50% probability.

**Table 1.** Selected Bond Lengths [Å] and angles [°] for the crystal structure of Ph-Pt.

Pt1–C15	1.970(9)	C15–Pt1–N3	175.3(3)
Pt1–N3	2.008(7)	C15–Pt1–C14	94.7(3)
Pt1–C14	2.012(9)	N3–Pt1–C14	82.3(3)
Pt1–N2	2.132(7)	C15–Pt1–N2	105.5(3)
Pt2–C39	1.965(8)	N3–Pt1–N2	77.5(3)
Pt2–C40	1.967(9)	C14–Pt1–N2	159.7(3)
Pt2–N6	2.016(7)	C39–Pt2–C40	95.9(3)
Pt2–N5	2.098(7)	C39–Pt2–N6	81.8(3)
		C39–Pt2–N5	159.1(3)
		C40–Pt2–N6	177.6(3)
		C40–Pt2–N5	104.9(3)
		N6–Pt2–N5	77.3(3)

bands situated from 244–350 nm for Ph-Pt can be ascribed to intra-ligand  $\pi(L) \rightarrow \pi^*(L)$  transitions; the weaker, lower-energy transition at 412 nm can be ascribed to a  $d\pi(Pt) \rightarrow \pi^*(L)$  metal-to-ligand (<sup>1</sup>MLCT) electronic transition. In case of P-Pt1, P-Pt2, and P-Pt3 complexes, the absorptions at 276 and 310 nm increase in intensity in proportion to the number of Pt<sup>II</sup> C<sup>^</sup>N<sup>^</sup>N<sup>^</sup> units attached to the porphyrin core (Figure 2); this occurs in both solvent systems. Furthermore, the Soret band is less intense and broadened for all derivatives, P-Pt1, P-Pt2, and P-Pt3, compared to their precursors 1P, 2P, and 3P respectively (Supporting Information, Figure S53). This effect is modest in MeCN but clearly significant in water/DMSO (97:3), indicating

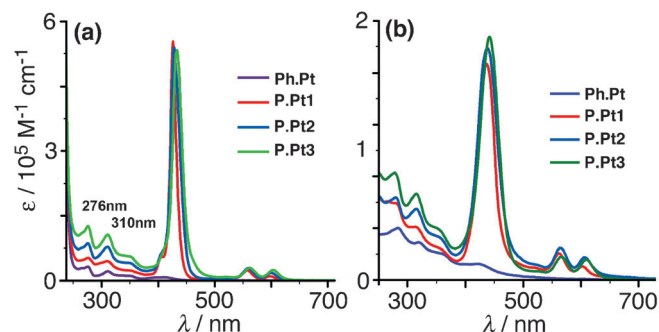


**Figure 2.** UV/Vis spectra of Ph-Pt, P-Pt1, P-Pt2, and P-Pt3 in a) MeCN and b) 3% DMSO in water, respectively. In the latter case the onset of aggregation broadens the peaks and makes measurements of the extinction coefficients unreliable.

that aggregation of the platinum-appended complexes occurs in the predominantly aqueous solvent. The extent of aggregation is maximum in case of **P-Pt1**, which contains the largest number of PEG chains in the series. Figure 3 shows the UV/Vis spectral changes of **P-Pt1** in different water/DMSO solvent mix-

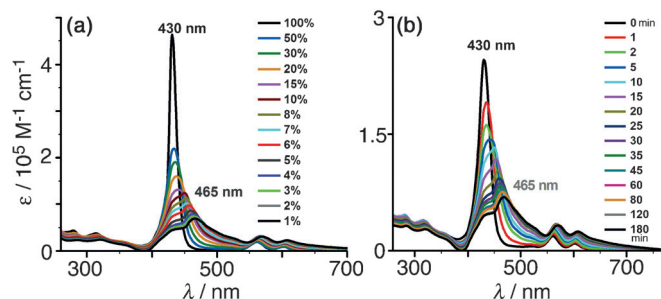


**Figure 3.** UV/Vis spectral changes in **P-Pt1**: a) upon increasing the proportion of water in the water/DMSO solvent mixture (% figures shown are % DMSO in the water/DMSO mixture); and b) with time, in 3% DMSO in water. Sample concentrations were  $5 \mu\text{M}$  in both cases.

tures with respect to time. It is clear that in predominantly aqueous media the intensity of the Soret band at 430 nm gradually decreases, with the concomitant generation of a shoulder near 465 nm as well as the generation of broad and overlapping Q-bands, suggesting that J-type aggregation of **P-Pt1** occurs under these solvent conditions.<sup>[15]</sup> As a control experiment we examined **Ph-Pt** on its own and found that it showed no significant aggregation effects in either MeCN or DMSO/water at the concentration range used for these experiments, with UV/Vis absorbance being linearly related to concentration between  $10^{-4}$  and  $10^{-6}$  M.

The occurrence of aggregation was also supported by SEM studies on the nature and morphology of the aggregated species formed by **P-Pt1**. As shown in Figure 4, deposition from a DMSO–D<sub>2</sub>O solvent mixture permits observation of nanometric spherical aggregates of 100–600 nm diameter which

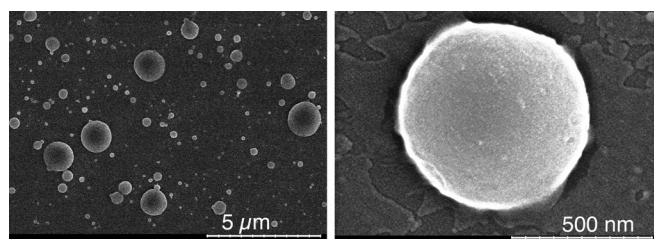


**Figure 4.** SEM images of **P-Pt1** indicating spherical aggregation of the molecules in DMSO–D<sub>2</sub>O solution. A magnified view is shown on the right.

supports the emergence of a new red-shifted shoulder on the Soret band: we suggest that this is due to J-aggregation<sup>[15]</sup> (Figure 2). The other compounds (**P-Pt2** and **P-Pt3**) aggregate relatively slowly compared to **P-Pt1** and did not produce any well-defined self-assembled structures that were visible by SEM experiments. Finally, we note that a gradual red-shift of the Soret band occurs from **P-Pt1** to **P-Pt3**, which shows that

increasing the number of alkynyl substituents reduces the energy required for the  $\pi$ – $\pi^*$  electronic transition.

### Luminescence properties

Luminescence spectra of the complexes were also measured in both MeCN and water/DMSO (97:3). The reference compound **Ph-Pt** in MeCN shows typical structured phosphorescence, with maxima at 514 and 543 nm and a lifetime of 77 ns, characteristic of luminescence from an  $^3\text{MLCT} \{d\pi(\text{Pt}) \rightarrow \pi^*(\text{L})\}$  excited state (Figure 5a).<sup>[12c–e]</sup> At 77 K, **Ph-Pt** shows a well-resolved

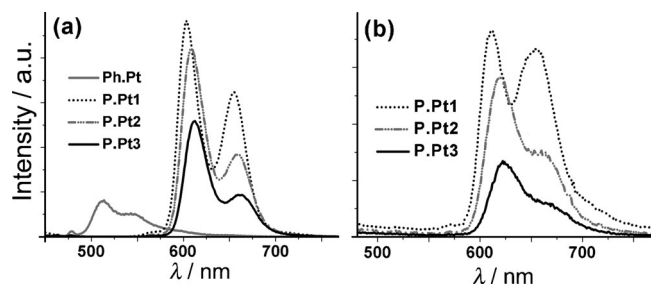


**Figure 5.** Emission spectra of **Ph-Pt**, **P-Pt1**, **P-Pt2**, and **P-Pt3** in a) MeCN and b) 3% DMSO in water. The concentration of all the compounds in MeCN are approximately  $2 \times 10^{-6}$  M and in 3% DMSO in water are ca.  $5 \times 10^{-6}$  M.  $\lambda_{\text{exc}} = 420$  nm in each case.

vibronically structured emission profile with peaks at 504, 542, and 582 nm. The rigidochromic shift of ca.  $400 \text{ cm}^{-1}$  of the highest-energy component on freezing is in agreement with a transition that contains some charge-transfer character; the mild solvent dependence at room temperature, with  $\lambda_{\text{em}}$  being blue-shifted by 15 nm with increasing solvent polarity (Supporting Information, Figure S54), is also consistent with this.

Luminescence spectra of **P-Ptn** in MeCN indicate that all three complexes exhibit near-complete quenching of the luminescence from the peripheral Pt<sup>II</sup> C<sup>^</sup>N<sup>^</sup>N<sup>^</sup> units at room temperature: only porphyrin-based luminescence was observed upon excitation at 420 nm for all three complexes, with quantum yield values slightly lower than those of the porphyrin precursors **nP** (Figure 5 and Table 2). This quenching of the peripheral groups could arise in principle from either photoinduced electron- or energy-transfer between the components. For electron-transfer, the available excited state energy from the Pt<sup>II</sup> C<sup>^</sup>N<sup>^</sup>N<sup>^</sup> unit is  $19800 \text{ cm}^{-1}$  (from the emission maximum at 77 K) which is 2.45 eV: this could be just sufficient to generate a charge-separated state based on the redox potentials of the component parts according to the Rehm–Weller equation (see electrochemical data below). However, the occurrence of photoinduced energy transfer as the quenching mechanism is unambiguously established from excitation spectra, which clearly showed that the absorption features from the Pt<sup>II</sup> units between 250 and 350 nm lead to sensitized Zn<sup>II</sup> porphyrin-based luminescence. The quantum yield of the porphyrin-based emission decreased with the increasing number of Pt<sup>II</sup> C<sup>^</sup>N<sup>^</sup>N<sup>^</sup> antenna groups (Table 2). Interestingly, the Pt<sup>II</sup>-based emission features of **P-Ptn** reappeared at low intensity in MeOH/EtOH frozen glasses at 77 K as a vibronic series cen-

**Table 2.** Photophysical data for the compounds used in the present study.

Compound	$\lambda_{\max}$ [nm]	$\epsilon$ [ $10^{-3}$ L mol $^{-1}$ cm $^{-1}$ ]	$\lambda_{\text{fl}}$ [nm]	$\Phi_{\text{fl}}$	$\tau/\text{ns}^{[\text{a}]}$	$\Phi_{\Delta}^{[\text{d}]}$
<b>1 P</b>	425 <sup>[a]</sup>	690 <sup>[c]</sup>	602, <sup>[a]</sup> 653 <sup>[a]</sup>	0.018 <sup>[a]</sup>	–	–
	428 <sup>[b]</sup>	250 <sup>[c]</sup>	–	–	–	–
<b>2 P</b>	425 <sup>[a]</sup>	720 <sup>[c]</sup>	603, <sup>[a]</sup> 655 <sup>[a]</sup>	0.019 <sup>[a]</sup>	–	–
	428 <sup>[b]</sup>	280 <sup>[c]</sup>	–	–	–	–
<b>3 P</b>	425 <sup>[a]</sup>	740 <sup>[c]</sup>	604, <sup>[a]</sup> 656 <sup>[a]</sup>	0.020 <sup>[a]</sup>	–	–
	428 <sup>[b]</sup>	290 <sup>[c]</sup>	–	–	–	–
<b>Ph-Pt</b>	276, <sup>[a]</sup> 311 <sup>[a]</sup>	32, 22	514, <sup>[a]</sup> 543 <sup>[a]</sup>	0.07 <sup>[a]</sup>	77	0.72
	283, <sup>[b]</sup> 320 <sup>[b]</sup>	– <sup>[e]</sup>	–	–	–	–
<b>P-Pt1</b>	426 <sup>[a]</sup>	550 <sup>[c]</sup>	603, <sup>[a]</sup> 655 <sup>[a]</sup>	0.014 <sup>[a]</sup>	2	0.63
	436 <sup>[b]</sup>	– <sup>[e]</sup>	612, <sup>[b]</sup> 657 <sup>[b]</sup>	– <sup>[e]</sup>	–	–
<b>P-Pt2</b>	428 <sup>[a]</sup>	540 <sup>[c]</sup>	608, <sup>[a]</sup> 658 <sup>[a]</sup>	0.010 <sup>[a]</sup>	2	0.59
	437 <sup>[b]</sup>	– <sup>[e]</sup>	619, <sup>[b]</sup> 664 <sup>[b]</sup>	– <sup>[e]</sup>	–	–
<b>P-Pt3</b>	433 <sup>[a]</sup>	530 <sup>[c]</sup>	612, <sup>[a]</sup> 662 <sup>[a]</sup>	0.006 <sup>[a]</sup>	2	0.55
	441 <sup>[b]</sup>	– <sup>[e]</sup>	623, <sup>[b]</sup> 670 <sup>[b]</sup>	– <sup>[e]</sup>	–	–

[a] Measurements were carried out in CH<sub>3</sub>CN. [b] Measurements were carried out in 3% DMSO in water. [c] The molar extinction coefficient values are at Soret bands. [d] Singlet oxygen measurements were carried out in CH<sub>2</sub>Cl<sub>2</sub>. [e] Extinction coefficients and fluorescence quantum yields were not measured in water/DMSO due to aggregation (see main text).

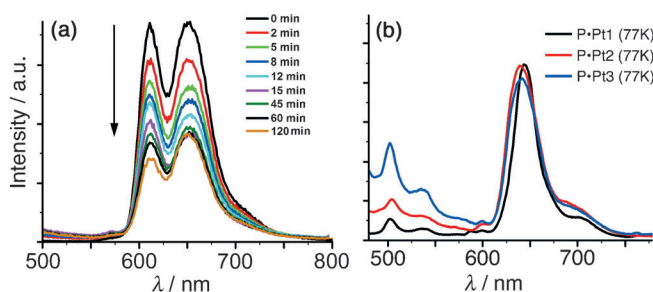


**Figure 6.** a) Emission spectral change of **P-Pt1** in 3% DMSO in water with respect to time. The concentration of **P-Pt1** complex is  $5 \times 10^{-6}$  M.  $\lambda_{\text{exc}} = 420$  nm during all the measurements. b) Emission spectra of **P-Pt1**, **P-Pt2**, and **P-Pt3** in MeOH/EtOH (1:4, v/v) as a frozen glass at 77 K.

tered around 502, 537, and 575 nm, respectively, indicating that EnT from Pt<sup>II</sup> C<sup>N</sup>N<sup>N</sup> antenna to porphyrin core is incomplete (Figure 6). These features are weak compared to the main porphyrin-centered emission; it may be that they are present at RT but too weak to see, with the usual intensity enhancement at low temperature making them just visible. In this case, energy-transfer is not 100% efficient: we cannot measure a lifetime for these weak features.

Using water/DMSO (97:3) as solvent, we could again see the aggregation that is present from the UV/Vis spectra, with emission spectra changing with time after dissolution (Figure 6a; Supporting Information, Figure S56). Gradual quenching of fluorescence with time was apparent in every case: among all these species **P-Pt1** shows fast aggregation compared to the others. For this reason we did not attempt to measure luminescence quantum yield values in this solvent.

### Singlet oxygen generation

The quantum yields for generation of singlet oxygen ( $\Phi_{\Delta}$ ) for these complexes were determined according to previous reports.<sup>[16]</sup> The quantum yield of <sup>1</sup>O<sub>2</sub> generation by **P-Ptn** along with that of the **Ph-Pt** reference were determined against the

standard phenalenone in DCM ( $\Phi_{\Delta} = 0.95$ ), by excitation at 355 nm with detection of phosphorescence from singlet oxygen at 1270 nm. The experimental results revealed that the highest efficiency of <sup>1</sup>O<sub>2</sub> generation is found for **P-Pt1** ( $\Phi_{\Delta} = 0.63$ ) among the series, which is reasonably comparable with other porphyrin-based systems reported recently.<sup>[49,6e]</sup> All of the photophysical data for the compounds are summarized in Table 2.

### Electrochemical properties

Cyclic voltammetry (CV) measurements on the complexes were performed in dichloromethane (DCM) and dimethylformamide (DMF) containing 0.1 M *tetra*-n-butylammonium hexafluorophosphate (TBAPF<sub>6</sub>) as supporting electrolyte under an argon atmosphere. The electrochemical data for all the references and the complexes are summarized in Table 3. The compounds, **1 P**, **2 P**, and **3 P** were measured under identical experi-

**Table 3.** Electrochemical data for the compounds used in present study.

Entity	$E_{\text{red}}^2$ [V]	$E_{\text{red}}^1$ [V]	$E_{\text{ox}}^1$ [V]	$E_{\text{ox}}^2$ [V]	$E_{\text{ox}}^3$ [V]
<b>1 P</b>	–1.65 <sub>r</sub> <sup>[a]</sup>	–1.41 <sup>[a]</sup>	+0.81 <sup>[a]</sup>	+1.14 <sup>[a]</sup>	–
<b>2 P</b>	–1.62 <sub>r</sub> <sup>[a]</sup>	–1.42 <sup>[a]</sup>	+0.79 <sup>[a]</sup>	+1.11 <sup>[a]</sup>	–
<b>3 P</b>	–1.68 <sup>[a]</sup>	–1.38 <sup>[a]</sup>	+0.84 <sup>[a]</sup>	+1.11 <sup>[a]</sup>	–
<b>Ph-Pt</b>	–	–1.77 <sub>r</sub> <sup>[a]</sup>	+0.97 <sub>r</sub> <sup>[a]</sup>	–	–
<b>P-Pt1</b>	–1.82 <sub>r</sub> <sup>[a]</sup>	–1.45 <sub>r</sub> <sup>[a]</sup>	+0.77 <sub>r</sub> <sup>[a]</sup>	+0.83 <sup>[a]</sup>	+1.17 <sup>[a]</sup>
	–1.48 <sup>[b]</sup>	–1.14 <sup>[b]</sup>	+1.01 <sub>r</sub> <sup>[b]</sup>	+1.12 <sub>r</sub> <sup>[b]</sup>	–
<b>P-Pt2</b>	–1.79 <sub>r</sub> <sup>[a]</sup>	–1.42 <sub>r</sub> <sup>[a]</sup>	+0.78 <sub>r</sub> <sup>[a]</sup>	+0.88 <sup>[a]</sup>	+1.20 <sup>[a]</sup>
	–1.45 <sup>[b]</sup>	–1.14 <sup>[b]</sup>	+0.99 <sub>r</sub> <sup>[b]</sup>	+1.12 <sub>r</sub> <sup>[b]</sup>	–
<b>P-Pt3</b>	–1.71 <sub>r</sub> <sup>[a]</sup>	–1.36 <sub>r</sub> <sup>[a]</sup>	+0.79 <sub>r</sub> <sup>[a]</sup>	+0.94 <sup>[a]</sup>	+1.23 <sup>[a]</sup>
	–1.44 <sup>[b]</sup>	–1.12 <sup>[b]</sup>	+1.04 <sub>r</sub> <sup>[b]</sup>	–	–

[a] Measurements were carried out in dry CH<sub>2</sub>Cl<sub>2</sub> or [b] dry DMF containing 0.1 M TBAPF<sub>6</sub> as the supporting electrolyte. Potentials are in V versus the Ag<sup>0</sup>/Ag<sup>+</sup> couple (silver wire) recorded under the conditions of analysis. The scan rate was 0.05 V s<sup>–1</sup>. Under these conditions, the ferrocene/ferrocenium couple occurred at +0.70 V in DMF and +0.50 V in CH<sub>2</sub>Cl<sub>2</sub>.

mental conditions to analyse the electrochemical results across the series of complexes (Supporting Information, Figure S58a).

The CV of the mononuclear reference complex **Ph-Pt** revealed completely irreversible behaviour at high positive/negative potentials (Table 3, Supporting Information, Figure S59a). In contrast all of the porphyrin reference compounds (with no Pt<sup>II</sup> C<sup>^</sup>N<sup>^</sup>N substituents) showed two reversible one-electron waves at positive potentials, associated with the porphyrin core, and one or two irreversible reductions at negative potentials. For the platinated complexes **P-Ptn**, we again see the features associated with the Zn<sup>II</sup> porphyrin core, but additional features on the outward sweep appeared at +0.77 V (**P-Pt1**), +0.78 V (**P-Pt2**), and +0.79 V (**P-Pt3**) in DCM solution, which correspond to the irreversible oxidation of the Pt<sup>II</sup> C<sup>^</sup>N<sup>^</sup>N group.

The electrochemical behaviour of **P-Ptn** in anhydrous DMF is somewhat different: the first reductive process at ca. -1.14 V now becomes a reversible one electron reduction process, which is equally intense for all three complexes (Figure 7), whereas the subsequent reduction is associated with the multiple overlapping redox processes from both porphyrin and the Pt<sup>II</sup> C<sup>^</sup>N<sup>^</sup>N moieties. We can see that the peak current of this reductive wave increases with the number of Pt<sup>II</sup> C<sup>^</sup>N<sup>^</sup>N units.

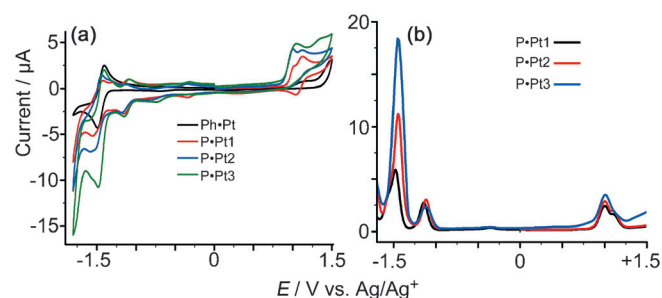


**Figure 7.** a) Cyclic voltammograms of **P-Pt1**, **P-Pt2**, **P-Pt3**, and **Ph-Pt**; and b) square-wave voltammograms of **P-Pt1**, **P-Pt2**, and **P-Pt3**. All measurements were carried out in anhydrous DMF containing 0.1 M TBAPF<sub>6</sub> as the supporting electrolyte under an Ar atmosphere. A platinum working and counter electrode, and a silver quasi-reference electrode were used during measurement. The scan rate was 0.05 V s<sup>-1</sup>.

Furthermore, there is a slight positive shift of the reduction potentials from **P-Pt1** (-1.82 V) to **P-Pt3** (-1.71 V) in both DCM and DMF, indicating that **P-Pt3** is the easiest to reduce among this series. There is a similar slight positive shift of first oxidation across the series, from +1.17 V (**P-Pt1**) to +1.23 V (**P-Pt3**) in DCM. Thus, an increasing number of conjugated alkynyl substituents from **P-Pt1** to **P-Pt3** results in the porphyrin core becoming slightly more electron-deficient, although the effect is relatively small, presumably because the *meso* phenyl substituents are orthogonal to the porphyrin plane which limits electronic communication between the components. Thus, the porphyrin and Pt<sup>II</sup> C<sup>^</sup>N<sup>^</sup>N units can be considered to be almost independent. The differential pulse voltammograms for the complexes (Figure 7b) clearly show the steady increase in current generated near reduction potential values of -1.45 V with the incremental addition of Pt<sup>II</sup> C<sup>^</sup>N<sup>^</sup>N moieties.

For individual CVs, see the Supporting Information, Figures S58–S60.

### Theoretical studies

In an effort to gain more insight for structures and photophysical properties of **P-Ptn**, density functional theory (DFT) calculations were performed using the Gaussian 09 program suite.<sup>[17]</sup> All of the calculations were carried out with Becke's three-parameter hybrid exchange functional (B3LYP);<sup>[18]</sup> a basis set of 6-31G\* was employed for H, C, N, and O atoms, and for Zn<sup>II</sup> and Pt<sup>II</sup> we used the LanL2DZ<sup>[19]</sup> basis set. The structures of the core porphyrin planes for **P-Ptn** were found to be nearly coplanar, and the Pt<sup>II</sup> C<sup>^</sup>N<sup>^</sup>N unit is lying in perpendicular to the *meso*-ethylphenyl bridge (Supporting Information, Figure S61). The torsion angles between the porphyrin plane and Pt<sup>II</sup> C<sup>^</sup>N<sup>^</sup>N unit are thus approximately 20° for all derivatives. The bond lengths around Pt<sup>II</sup> center of **P-Pt1** are also consistent with the crystal structure of **Ph-Pt** (for example, Pt–C<sub>alkynyl</sub> = 1.969, Pt–N<sub>pyridine</sub> = 2.048, Pt–C<sub>phenyl</sub> = 1.992, Pt–N<sub>pyrazole</sub> = 2.221 Å) with the bond to the anionic C donor being characteristically shorter than the Pt–N bonds. For the other derivatives, **P-Pt2** and **P-Pt3**, the coordination geometry does not change significantly upon increasing the number of Pt<sup>II</sup> C<sup>^</sup>N<sup>^</sup>N units.

The frontier molecular orbitals of **P-Ptn** obtained from time-dependent DFT (B3LYP) were examined (Figure 8; Supporting Information, Figure S62–S64, Tables S2–S4). For **P-Pt1**, it is noted that the absorption bands are dominated by the typical porphyrin-based MO interactions (that is, presence of a Soret

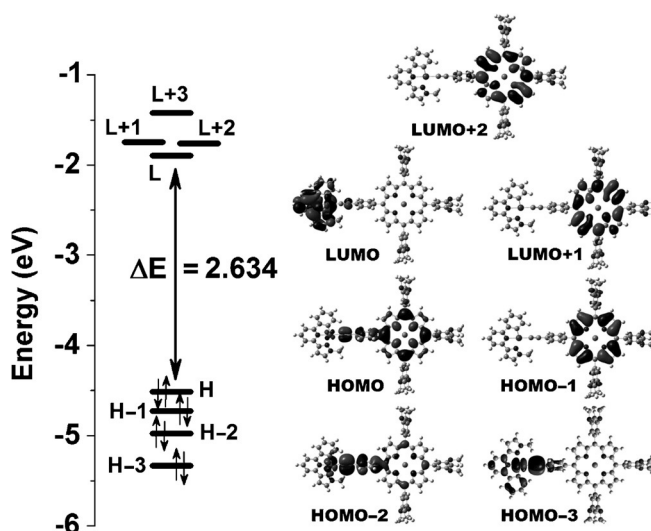


**Figure 8.** Molecular orbital energy level diagram and selected density maps of frontier orbitals of **P-Pt1** (For details, see the Supporting Information).

and Q-bands); hence the spectral feature is interpreted by Gouterman's four-orbital model. The HOMO and HOMO–1 are composed of the porphyrin-based  $\pi$  orbitals with  $a_{1u}$  and  $a_{2u}$  symmetries, respectively, along with the contribution of the  $\text{C}\equiv\text{C}$  alkynyl side group. The LUMO+1 and LUMO+2 are dominant by the degenerate  $e_g$  symmetric orbitals. In the LUMO, the main electron density is delocalized on the Pt<sup>II</sup>

C<sup>^</sup>N<sup>^</sup>N unit, which is closely lying with the degenerated LUMO+1 and LUMO+2. The lowest energy HOMO–LUMO transition can be considered as an intramolecular charge transfer (ICT), which is less contributed to the actual spectrum (Supporting Information, Figure S66–S68).

Similar to **P-Pt1**, the MO distributions for **P-Pt2** and **P-Pt3** could be understood by integration of the additional MOs of the Pt<sup>II</sup> (C<sup>^</sup>N<sup>^</sup>N) unit lying between the pairs of four orbitals of the porphyrin (HOMO/HOMO–1 and LUMO+[*m*]/LUMO+[*m*+1]; where *m*=2 and 3, respectively) given in the Supporting Information, Figure S62 and S63, respectively. The energies of HOMOs for **P-Pt2** and **P-Pt3** are destabilized by increasing the number of Pt<sup>II</sup> C<sup>^</sup>N<sup>^</sup>N units due to the  $\pi$ -extension through the C $\equiv$ C alkynyl bridges. Therefore, the HOMO–LUMO gap ( $\Delta E$ , eV) are systematically decreased upon installing the Pt<sup>II</sup> units, which is in agreement of the slight redshift of the absorption bands (Supporting Information, Figure S65).

## Conclusion

We have synthesized a series of new porphyrins that combine a Zn<sup>II</sup> tetraphenylporphyrin core and one, two, or three pendant cyclometalated Pt<sup>II</sup> C<sup>^</sup>N<sup>^</sup>N units which are attached through the *meso* positions. Water solubility is assisted by the presence of PEG groups, although this was not completely successful in making the complexes water-soluble, as aggregation occurred in water/DMSO mixtures; unfortunately this prevented use of the complexes as cell imaging agents. The effect of incremental addition of Pt<sup>II</sup> C<sup>^</sup>N<sup>^</sup>N groups is reflected in their electrochemical and spectroscopic behavior. In all cases the characteristic phosphorescence of the Pt<sup>II</sup> C<sup>^</sup>N<sup>^</sup>N groups is quenched by efficient energy-transfer to the Zn<sup>II</sup> porphyrin core which has a lower-energy emissive excited state. All these Zn<sup>II</sup> porphyrin–Pt<sup>II</sup> C<sup>^</sup>N<sup>^</sup>N acetylides are effective photosensitizers for singlet oxygen generation. Such porphyrin-based architectures, with improved solubility, could also offer significant possibilities for bio-imaging.

## Experimental Section

### Materials

All reagents and starting materials were purchased from Aldrich Chemical Co. and were used as received. 3,5-bis(9-methoxy-1,4,7-trioxanonyl)phenylaldehyde was synthesized using the previously reported procedure.<sup>[13b,20]</sup> All anhydrous solvents were acquired from Aldrich Chemical Co. and used without further purification. All reactions were carried out under an argon atmosphere unless noted otherwise. Chromatographic separations were performed by means of column chromatography by using 100–200 mesh silica gel obtained from Merck. Final separation of the compounds was performed by a long sephadex-LH20 column using CHCl<sub>3</sub> as eluent.

### Instruments

<sup>1</sup>H (500 MHz) and <sup>13</sup>C (125 MHz) NMR spectra were recorded using a Bruker DPX-500 spectrometer in CDCl<sub>3</sub> or CD<sub>3</sub>OD at 298 K using either residual solvent signals or tetramethylsilane as internal

standards. ESI-MS were recorded using a Micromass LCT instrument. MALDI-TOF mass spectra were recorded using a Bruker Microflex 2 LRF 20 spectrometer with dithranol (1,8,9-trihydroxyanthracene) as a matrix. UV/Vis spectra were recorded using a Varian Cary 50 spectrophotometer at 298 K (solvent as given in Table 2). Luminescence spectra were measured on a Jobin Yvon Fluoromax 4 fluorimeter. Emission lifetime values were measured using the time-correlated single photon counting (TCSPC) technique with an Edinburgh Instruments "Mini  $\tau$ " spectrometer, equipped with a 410 nm pulsed diode laser as an excitation source and a Hamamatsu H577303 photomultiplier tube (PMT) detector. The lifetimes were calculated from the measured data using the supplied software. Voltammetric measurements were carried out with an Autolab PGSTAT-100 electrochemical workstation with Pt working/counter electrodes, and an Ag wire pseudo-reference electrode, in dichloromethane (DCM) that contained 0.1 M TBAPF<sub>6</sub> as base electrolyte, under an Ar atmosphere. Ferrocene (Fc) was added as an internal reference. Potentials are reported versus the Ag<sup>0</sup>/Ag<sup>+</sup> couple. The concentration of all compounds analyzed was 10<sup>–4</sup> M in solvents used.

### X-ray crystal structure determination

Single crystals of **Ph-Pt** grew as orange needles by slow evaporation from CHCl<sub>3</sub> in the presence of diethyl ether. The data were collected using a Bruker SMART-APEX2 CCD diffractometer using graphite-monochromated Mo-K $\alpha$  radiation ( $\lambda$ =0.71073 Å) from a sealed-tube source. The data were collected at 293 K. Details of crystal data, data collection, and structure refinement are listed in the Supporting Information (Tables S4, S5, S6, and S7, respectively). After integration of the raw data, and before merging, an empirical absorption correction was applied (SADABS)<sup>[21]</sup> based on comparison of multiple symmetry-equivalent measurements. The structures were solved by direct methods and refined by full-matrix least squares on weighted *F*<sup>2</sup> values with anisotropic displacement parameters for the non-hydrogen using the SHELX suite of programs.<sup>[22]</sup> Structure analysis was aided by use of the WinGX<sup>[23]</sup> program. Neutral atom scattering factors and values used to calculate the linear absorption coefficient are from the International Tables for X-ray Crystallography (1992).<sup>[24]</sup> CCDC 1424398 contains the supplementary crystallographic data for this paper. These data can be obtained free of charge from The Cambridge Crystallographic Data Centre.

### SEM experiment

Scanning electron microscopy was carried out using a Hitachi S-4800 FE-SEM at an accelerating voltage of 5 kV on the samples cast on silicon substrates. Samples for SEM measurements were prepared by injecting a 0.5 mg mL<sup>–1</sup> solution of the compounds in dimethylsulfoxide (10  $\mu$ L) into water (0.5 mL). An aliquot of sample was dropped from a Pasteur pipette onto a clean silicon substrate and dried in vacuo prior to coating. Samples were coated with platinum (ca. 5 nm) using a Hitachi S-1050 vacuum coater.

### Theoretical calculations

All calculations were carried out using the Gaussian09 program package.<sup>[17]</sup> The 6-31G\* basis set was employed for all atoms except Pt, which was described by the Stuttgart small-core relativistic effective-core potential, LanL2DZ with its accompanying basis set.<sup>[19]</sup> The Becke three-parameter hybrid exchange functional and the Lee–Yang–Parr correlation functional (B3LYP) were employed for all DFT calculations.<sup>[18]</sup> The PEG chains were replaced by OMe

groups and the propyl groups on C<sup>N</sup>N ligand are replaced by Me groups to minimize the computational cost of time during geometrical optimization. Based on the optimized geometries in the gas phase, the TD-DFT calculations at the same level was employed to study the nature of transitions in the absorption spectra.

### Synthesis of porphyrins

The key porphyrin precursors were synthesized by mixing pyrrole, and two different aldehydes in an appropriate ratio in anhydrous CH<sub>2</sub>Cl<sub>2</sub>.

**A) Synthesis of porphyrins by Lindsey's method:** The mixed porphyrin precursors **1PH2** and **3PH2** were synthesized by following standard Lindsey technique.<sup>[14]</sup> Typically this was carried out by taking freshly distilled pyrrole (0.278 mL, 4 mmol), 3,5-bis(9-methoxy-1,4,7-trioxanonyl)phenylaldehyde (1.291 g, 3 mmol), and 4-[(Trimethylsilyl)ethynyl]benzaldehyde (0.2023 g, 1 mmol) in a clean and dry 1 L three-necked round-bottomed flask under an argon atmosphere. anhydrous DCM (700 mL) was added to this and purged with argon for ca. 30 min at room temperature with constant stirring. Thereafter, a catalytic amount of BF<sub>3</sub>·OEt<sub>2</sub> was added to this and stirred the reaction mixture vigorously overnight at RT. The red color generates very slowly, which darkens after 2–3 h. DDQ (1.816 g, 8 mmol) was added gradually to this deep red solution and stirred for another 3 h at RT followed by the addition of triethylamine (2 mL) to neutralize the dark reaction mixture. Evaporation of the reaction mixture under reduced pressure and purification by flash column chromatography using CH<sub>2</sub>Cl<sub>2</sub> as eluent afforded various types of mixed porphyrins in moderate to good yield. Generally, multiple rounds of column chromatographic separations are required to purify each different porphyrins. From this method the bis-derivatives contains both *cis* and *trans* isomers, which are almost inseparable, and thus to make the *trans* derivative (**2PH2**) we used directional synthesis by using 4-[(trimethylsilyl)ethynyl]phenyl-dipyrrole as precursor.

Typically, this was carried out by following the same procedure as described above but taking 4-[(trimethylsilyl)ethynyl]phenyl dipyrromethane (0.636 g, 2 mmol) and 3,5-bis(9-methoxy-1,4,7-trioxanonyl)phenylaldehyde (0.861 g, 2 mmol) to obtain exclusively the *trans* product.

**1PH2:** Yield ca. 20%; <sup>1</sup>H NMR (500 MHz, CDCl<sub>3</sub>, 298 K, TMS): δ = –2.85 (s, 2H), 0.38 (s, 9H), 3.31 (s, 18H), 3.48–3.50 (m, 12H), 3.61–3.63 (m, 12H), 3.68–3.70 (m, 12H), 3.76–3.78 (m, 12H), 3.92–3.95 (m, 12H), 4.29–4.31 (m, 12H), 6.94–6.95 (m, 3H), 7.40 (d, *J* = 2.2 Hz, 6H), 7.88 (d, *J* = 8.2 Hz, 2H), 8.16 (d, *J* = 8.2 Hz, 2H), 8.79 (d, *J* = 4.8 Hz, 2H), 8.91 (s, 4H), 8.92 ppm (d, *J* = 4.8 Hz, 2H); <sup>13</sup>C NMR spectra (125 MHz, CDCl<sub>3</sub>, 298 K, TMS): δ = 0.1, 59.0, 67.8, 69.8, 70.6, 70.7, 70.9, 71.9, 95.5, 101.4, 105.1, 114.7, 119.2, 119.8, 119.9, 122.6, 130.4, 131.2, 134.4, 142.5, 143.8, 158.0 ppm; MALDI-TOF-MS: *m/z* calcd for C<sub>91</sub>H<sub>122</sub>N<sub>4</sub>O<sub>24</sub>Si: 1684.0; found: 1683.9 (100%).

**2PH2:** Yield ca. 25%; <sup>1</sup>H NMR (500 MHz, CDCl<sub>3</sub>, 298 K, TMS): δ = –2.84 (s, 2H), 0.39 (s, 18H), 3.31 (s, 12H), 3.48–3.50 (m, 8H), 3.61–3.63 (m, 8H), 3.68–3.70 (m, 8H), 3.76–3.78 (m, 8H), 3.92–3.94 (m, 8H), 4.29–4.31 (m, 8H), 6.94 (t, *J* = 2.2 Hz, 2H), 7.40 (d, *J* = 2.2 Hz, 4H), 7.88 (d, *J* = 8.2 Hz, 4H), 8.16 (d, *J* = 8.2 Hz, 4H), 8.8 (d, *J* = 4.7 Hz, 4H), 8.94 ppm (d, *J* = 4.7 Hz, 4H); <sup>13</sup>C NMR spectra (125 MHz, CDCl<sub>3</sub>, 298 K, TMS): δ = 0.1, 59.0, 67.8, 69.8, 70.6, 70.7, 70.9, 71.9, 95.6, 101.4, 105.0, 114.7, 119.3, 120.0, 122.6, 130.4, 134.4, 142.4, 143.8, 158.0 ppm; MALDI-TOF-MS: *m/z* calcd for C<sub>82</sub>H<sub>102</sub>N<sub>4</sub>O<sub>16</sub>Si<sub>2</sub>: 1455.9; found: 1455.6 (100%).

**3PH2:** Yield ca. 18%; <sup>1</sup>H NMR (500 MHz, CDCl<sub>3</sub>, 298 K, TMS): δ = –2.84 (s, 2H), 0.38 (s, 27H), 3.31 (s, 6H), 3.48–3.50 (m, 4H), 3.61–3.63 (m, 4H), 3.67–3.69 (m, 4H), 3.75–3.77 (m, 4H), 3.92–3.93 (m,

4H), 4.28–4.30 (m, 4H), 6.94 (t, *J* = 2.2 Hz, 1H), 7.39 (d, *J* = 2.2 Hz, 2H), 7.87 (dd, *J* = 8.3 Hz, *J* = 2.2 Hz, 6H), 8.15 (dd, *J* = 8.2 Hz, *J* = 1.3 Hz, 6H), 8.80 (d, *J* = 4.8 Hz, 2H), 8.81 (s, 4H), 8.94 ppm (d, *J* = 4.7 Hz, 2H); <sup>13</sup>C NMR spectra (125 MHz, CDCl<sub>3</sub>, 298 K, TMS): δ = 0.1, 59.0, 67.8, 69.8, 70.6, 70.7, 70.9, 71.9, 95.6, 101.4, 105.0, 114.7, 119.5, 120.2, 122.7, 130.4, 131.0, 134.4, 142.3, 143.7, 158.0 ppm; MALDI-TOF-MS: *m/z* calcd for C<sub>73</sub>H<sub>82</sub>N<sub>4</sub>O<sub>8</sub>Si<sub>3</sub>: 1227.7; found: 1227.6 (100%).

**B) Synthesis of zinc(II) porphyrins:** Typically this was carried out by taking 0.1 mmol solution of the free base porphyrins (0.1684 g for **1PH2**, 0.1456 g for **2PH2**, and 0.1227 g for **3PH2**) in 200 mL CHCl<sub>3</sub> and MeOH (10:1 v/v) and Zn(OAc)<sub>2</sub> (0.1835 g, 1 mmol) in a clean dry two-necked round-bottomed flask. The mixtures were then refluxed for 4 h at 80 °C with constant stirring. The solvents were removed under reduced pressure and the products were extracted with CH<sub>2</sub>Cl<sub>2</sub> and washed with water, dried over MgSO<sub>4</sub>, filtered, and concentrated to near-dryness. The residue was then purified by column chromatography on Al<sub>2</sub>O<sub>3</sub> using CH<sub>2</sub>Cl<sub>2</sub>/MeOH; 99:1 as eluent to afford corresponding Zn<sup>II</sup> porphyrins (**1PZn**, **2PZn**, and **3PZn**) in good yield.

**1PZn:** Yield ca. 95%; <sup>1</sup>H NMR (500 MHz, CDCl<sub>3</sub>, 298 K, TMS): δ = 0.38 (s, 9H), 2.92 (s, 18H), 3.07–3.09 (m, 12H), 3.26–3.29 (m, 12H), 3.50–3.53 (m, 12H), 3.63–3.66 (m, 12H), 3.83–3.87 (m, 12H), 4.24–4.28 (m, 12H), 6.88 (t, *J* = 2.1 Hz, 2H), 6.90 (t, *J* = 2.1 Hz, 3H), 7.41–7.42 (m, 6H), 7.87 (d, *J* = 8.1 Hz, 2H), 8.16 (d, *J* = 8.1 Hz, 2H), 8.85 (d, *J* = 4.6 Hz, 2H), 8.96 (s, 4H), 8.98 ppm (d, *J* = 4.6 Hz, 2H); <sup>13</sup>C NMR spectra (125 MHz, CDCl<sub>3</sub>, 298 K, TMS): δ = 0.1, 58.5, 67.8, 69.8, 70.1, 70.4, 70.7, 71.3, 95.2, 101.3, 105.2, 114.7, 119.8, 120.6, 122.1, 130.1, 131.4, 131.8, 131.9, 134.3, 143.4, 144.6, 149.6, 149.7, 149.8, 149.9, 157.7 ppm; MALDI-TOF-MS: *m/z* calcd for C<sub>91</sub>H<sub>120</sub>N<sub>4</sub>O<sub>24</sub>SiZn: 1747.4; found: 1747.1 (100%).

**2PZn:** Yield ca. 92%; <sup>1</sup>H NMR (500 MHz, CDCl<sub>3</sub>, 298 K, TMS): δ = 0.38 (s, 18H), 2.82 (s, 12H), 2.98–2.99 (m, 8H), 3.18–3.20 (m, 8H), 3.45–3.47 (m, 8H), 3.59–3.60 (m, 8H), 3.79–3.81 (m, 8H), 4.21–4.23 (m, 8H), 6.86 (s, 2H), 7.41 (d, *J* = 2.1 Hz, 4H), 7.87 (d, *J* = 8.1 Hz, 4H), 8.15 (d, *J* = 8.1 Hz, 4H), 8.86 (d, *J* = 4.6 Hz, 4H), 8.99 ppm (d, *J* = 4.6 Hz, 4H); <sup>13</sup>C NMR spectra (125 MHz, CDCl<sub>3</sub>, 298 K, TMS): δ = 0.1, 58.5, 67.9, 69.9, 70.1, 70.5, 70.7, 71.3, 95.3, 101.5, 105.2, 114.8, 120.1, 120.9, 122.3, 130.2, 131.6, 132.2, 134.3, 143.4, 144.6, 149.8, 157.8 ppm; MALDI-TOF-MS: *m/z* calcd for C<sub>82</sub>H<sub>100</sub>N<sub>4</sub>O<sub>16</sub>Si<sub>2</sub>Zn: 1519.2; found: 1519.9 (100%).

**3PZn:** Yield ca. 95%; <sup>1</sup>H NMR (500 MHz, CDCl<sub>3</sub>, 298 K, TMS): δ = 0.39 (s, 27H), 2.65 (s, 6H), 2.79–2.81 (m, 4H), 3.02–3.04 (m, 4H), 3.36–3.38 (m, 4H), 3.52–3.54 (m, 4H), 3.74–3.76 (m, 4H), 4.18–4.20 (m, 4H), 6.83 (t, *J* = 2.2 Hz, 1H), 7.41 (d, *J* = 2.2 Hz, 2H), 7.87 (dd, *J* = 8.2 Hz, *J* = 1.5 Hz, 6H), 8.16 (dd, *J* = 8.2 Hz, *J* = 1.4 Hz, 6H), 8.88 (d, *J* = 4.6 Hz, 2H), 8.90 (s, 4H), 8.99 ppm (d, *J* = 4.6 Hz, 2H); <sup>13</sup>C NMR spectra (125 MHz, CDCl<sub>3</sub>, 298 K, TMS): δ = 0.1, 58.4, 67.9, 69.8, 69.9, 70.4, 70.7, 71.1, 95.4, 101.6, 105.2, 114.8, 120.3, 121.1, 122.3, 130.2, 131.8, 132.3, 134.3, 143.3, 144.5, 149.8, 149.9, 150.0, 157.8 ppm; MALDI-TOF-MS: *m/z* calcd for C<sub>73</sub>H<sub>80</sub>N<sub>4</sub>O<sub>8</sub>Si<sub>3</sub>Zn: 1291.1; found: 1291.7 (100%).

**C) Desilylation of zinc(II) porphyrins:** K<sub>2</sub>CO<sub>3</sub> (83 mg, 0.6 mmol) was added to a solution of 0.1 mmol of each of the Zn<sup>II</sup> porphyrins (0.1747 g for **1PZn**, 0.1519 g for **2PZn**, and 0.1291 g of **3PZn**) in 200 mL anhydrous CHCl<sub>3</sub> and MeOH (3:1). The mixtures were stirred overnight at room temperature. The solvents were then removed under reduced pressure and the products extracted with CH<sub>2</sub>Cl<sub>2</sub> and washed with 10% NaHCO<sub>3</sub> solution. The organic fractions were dried over MgSO<sub>4</sub>, filtered and concentrated to near-dryness. Finally, the individual residues were purified by flash column chromatography, Al<sub>2</sub>O<sub>3</sub> (Brockmann type III) (CH<sub>2</sub>Cl<sub>2</sub>/MeOH, 99:1) to afford **1P**, **2P**, and **3P**, respectively.

**1P:** Yield ca. 90%;  $^1\text{H}$  NMR (500 MHz,  $\text{CDCl}_3$ , 298 K, TMS):  $\delta$  = 2.91 (s, 12H), 2.93 (s, 6H), 3.05–3.07 (m, 8H), 3.08–3.10 (m, 4H), 3.24–3.26 (m, 8H), 3.27–3.29 (m, 5H), 3.46–3.48 (m, 8H), 3.49–3.51 (m, 4H), 3.59–3.61 (m, 8H), 3.62–3.64 (m, 4H), 3.80–3.82 (m, 8H), 3.83–3.85 (m, 4H), 4.22–4.23 (m, 8H), 4.24–4.26 (m, 4H), 6.86 (t,  $J$  = 2.2 Hz, 2H), 6.89 (t,  $J$  = 2.2 Hz, 1H), 7.40–7.41 (m, 6H), 7.86 (d,  $J$  = 8.1 Hz, 2H), 8.17 (d,  $J$  = 8.2 Hz, 2H), 8.86 (d,  $J$  = 4.6 Hz, 2H), 8.96 (s, 4H), 8.98 ppm (d,  $J$  = 4.6 Hz, 2H);  $^{13}\text{C}$  NMR spectra (125 MHz,  $\text{CDCl}_3$ , 298 K, TMS):  $\delta$  = 58.5, 67.7, 69.7, 69.8, 70.0, 70.1, 70.3, 70.4, 70.6, 70.7, 71.3, 71.4, 78.1, 83.7, 101.2, 114.7, 119.6, 120.6, 121.1, 130.2, 131.4, 131.8, 131.9, 134.3, 143.7, 144.7, 149.6, 149.7, 149.8, 149.9, 157.7 ppm; MALDI-TOF-MS:  $m/z$  calcd for  $\text{C}_{88}\text{H}_{112}\text{N}_4\text{O}_{24}\text{Zn}$ : 1675.2; found: 1675.9 (100%).

**2P:** Yield ca. 87%;  $^1\text{H}$  NMR (500 MHz,  $\text{CDCl}_3$ , 298 K, TMS):  $\delta$  = 2.85 (s, 12H), 3.02 (t,  $J$  = 4.6 Hz, 8H), 3.22 (t,  $J$  = 4.4 Hz, 8H), 3.29 (s, 2H), 3.50 (t,  $J$  = 4.7 Hz, 8H), 3.63 (t,  $J$  = 4.4 Hz, 8H), 3.84 (t,  $J$  = 4.4 Hz, 8H), 4.25 (t,  $J$  = 4.3 Hz, 8H), 6.88 (s, 2H), 7.43 (s, 4H), 7.87 (d,  $J$  = 7.5 Hz, 4H), 8.16 (d,  $J$  = 7.5 Hz, 4H), 8.87 (d,  $J$  = 4.4 Hz, 4H), 8.99 ppm (d,  $J$  = 4.4 Hz, 4H);  $^{13}\text{C}$  NMR spectra (125 MHz,  $\text{CDCl}_3$ , 298 K, TMS):  $\delta$  = 58.6, 67.9, 69.9, 70.1, 70.5, 70.8, 71.4, 78.1, 83.8, 101.6, 114.8, 120.0, 120.9, 121.3, 130.3, 131.6, 132.2, 134.4, 143.6, 144.5, 149.8, 149.9, 157.8 ppm; MALDI-TOF-MS:  $m/z$  calcd for  $\text{C}_{76}\text{H}_{84}\text{N}_4\text{O}_{16}\text{Zn}$ : 1374.9; found: 1374.7 (100%).

**3P:** Yield ca. 88%;  $^1\text{H}$  NMR (500 MHz,  $\text{CDCl}_3$ , 298 K, TMS):  $\delta$  = 2.64 (s, 6H), 2.78 (t,  $J$  = 5.0 Hz, 4H), 3.00 (t,  $J$  = 4.7 Hz, 4H), 3.27 (s, 1H), 3.28 (s, 2H), 3.32 (t,  $J$  = 5.0 Hz, 4H), 3.48 (t,  $J$  = 5.0 Hz, 4H), 3.71 (t,  $J$  = 4.7 Hz, 4H), 4.16 (t,  $J$  = 4.5 Hz, 4H), 6.82 (t,  $J$  = 2.2 Hz, 1H), 7.41 (d,  $J$  = 1.9 Hz, 2H), 7.85–7.87 (m, 6H), 8.17 (d,  $J$  = 7.8 Hz, 6H), 8.89 (d,  $J$  = 4.6 Hz, 2H), 8.91 (s, 4H), 9.01 ppm (d,  $J$  = 4.6 Hz, 2H);  $^{13}\text{C}$  NMR spectra (125 MHz,  $\text{CDCl}_3$ , 298 K, TMS):  $\delta$  = 58.3, 67.8, 69.7, 69.8, 70.3, 70.6, 71.0, 78.1, 83.7, 101.5, 114.8, 120.1, 121.1, 121.3, 130.3, 131.7, 131.8, 132.3, 134.3, 143.5, 144.4, 149.7, 149.8, 149.9, 150.0, 157.8 ppm; MALDI-TOF-MS:  $m/z$  calcd for  $\text{C}_{64}\text{H}_{56}\text{N}_4\text{O}_8\text{Zn}$ : 1074.5; found: 1074.3 (100%).

**D) Synthesis of the  $\text{C}^{\wedge}\text{N}^{\wedge}\text{NNPr}$  ligand:** The  $\text{C}^{\wedge}\text{N}^{\wedge}\text{NNH}$  ligand was prepared by following the previously reported method.<sup>[25]</sup> Then the  $\text{C}^{\wedge}\text{N}^{\wedge}\text{NNPr}$  ligand was prepared by the standard substitution method.<sup>[12d]</sup> 2-Phenyl-6-(1*H*-pyrazol-3-yl)pyridine (1.1 g, 5 mmol) and NaH (60% by weight dispersed in mineral oil), (0.24 g, 6 mmol) was taken in a 250 mL two-necked round-bottomed flask, which was evacuated and back-filled with Ar several times. Anhydrous THF (100 mL) was added to this and stirred for 1 h at RT. Propyl bromide (0.91 mL, 10 mmol) was injected slowly to this reaction mixture and heated at 70 °C with constant stirring for overnight. White solids were filtered off under vacuum. The brown solvent mixture was evaporated under reduced pressure and the crude product was purified by silica gel column chromatography using hexane/diethyl ether (2:1) as the eluent to give 1.4 g of the colorless semisolid materials.

**$\text{C}^{\wedge}\text{N}^{\wedge}\text{NNPr}$ :** Yield ca. 87%;  $^1\text{H}$  NMR (400 MHz,  $\text{CDCl}_3$ , 298 K, TMS):  $\delta$  = 0.98 (t,  $J$  = 7.4 Hz, 3H), 1.97 (sextet,  $J$  = 7.3 Hz, 2H), 4.17 (t,  $J$  = 7.2 Hz, 2H), 7.10 (d,  $J$  = 2.3 Hz, 1H), 7.45–7.47 (m, 2H), 7.52 (t,  $J$  = 7.6 Hz, 2H), 7.67 (dd,  $J$  = 7.8 Hz,  $J$  = 0.8 Hz, 1H), 7.79 (t,  $J$  = 7.8 Hz, 1H), 7.97 (dd,  $J$  = 7.8 Hz,  $J$  = 0.8 Hz, 1H), 8.16 ppm (dd,  $J$  = 7.1 Hz,  $J$  = 1.4 Hz, 2H);  $^{13}\text{C}$  NMR spectra (100 MHz,  $\text{CDCl}_3$ , 298 K, TMS):  $\delta$  = 11.2, 23.9, 54.2, 104.5, 118.2, 118.8, 127.0, 128.6, 128.9, 130.5, 137.2, 139.5, 152.0, 152.3, 156.6 ppm; ESI-MS:  $m/z$  calcd for  $\text{C}_{17}\text{H}_{17}\text{N}_3$ : 263.3; found: 264.2 (100%).

**E) Synthesis of the  $\text{Pt}(\text{C}^{\wedge}\text{N}^{\wedge}\text{N})\text{Cl}$  complex:** In a 100 mL two-necked clean and dry round-bottomed flask,  $\text{C}^{\wedge}\text{N}^{\wedge}\text{NNPr}$  ligand (0.5267 g, 2 mmol) and  $\text{K}_2\text{PtCl}_4$  (0.7887 g, 1.9 mmol) was added under an argon atmosphere. Then degassed HOAc (50 mL) was added to this reaction mixture and heated at 110–115 °C for 2 days

with vigorous stirring. The progress of the reaction was monitored by taking small aliquots and treating them with  $\text{H}_2\text{O}$ . The appearance of a red color indicated the presence of unreacted  $\text{K}_2\text{PtCl}_4$ . After 2 days, the starting  $\text{Pt}^{\text{II}}$  salt was completely consumed and the mixture was allowed to cool to 0 °C. The resulting bright yellow crystalline complex was filtered off and washed with  $\text{H}_2\text{O}$  and  $\text{Et}_2\text{O}$  to give 1.35 g of the crude  $\text{Pt}^{\text{II}}$  complex as a bright yellow solid mass. The crude product was then purified by column chromatography using silica gel with 100% DCM as eluent.

Yield ca. 78%;  $^1\text{H}$  NMR (500 MHz,  $\text{CDCl}_3$ , 298 K, TMS):  $\delta$  = 0.98 (t,  $J$  = 7.4 Hz, 3H), 1.99 (sextet,  $J$  = 7.3 Hz, 2H), 4.59 (t,  $J$  = 7.2 Hz, 2H), 6.64 (d,  $J$  = 2.6 Hz, 1H), 7.05 (td,  $J$  = 7.5 Hz,  $J$  = 1.2 Hz, 1H), 7.18 (td,  $J$  = 7.5 Hz,  $J$  = 1.4 Hz, 1H), 7.23 (dd,  $J$  = 7.8 Hz,  $J$  = 1.0 Hz, 1H), 7.27 (dd,  $J$  = 7.6 Hz,  $J$  = 1.4 Hz, 1H), 7.34 (d,  $J$  = 8.2 Hz,  $J$  = 1.0 Hz, 1H), 7.53 (d,  $J$  = 2.6 Hz, 1H), 7.71 (t,  $J$  = 7.9 Hz, 1H), 7.79 ppm (dd,  $J$  = 7.7 Hz,  $J$  = 0.9 Hz, 1H);  $^{13}\text{C}$  NMR spectra (125 MHz,  $\text{CDCl}_3$ , 298 K, TMS):  $\delta$  = 10.9, 24.3, 54.4, 105.0, 115.8, 116.3, 124.0, 124.1, 130.7, 132.4, 133.9, 138.4, 138.8, 145.8, 150.7, 152.6, 166.5 ppm; ESI-MS:  $m/z$  calcd for  $\text{C}_{17}\text{H}_{16}\text{N}_3\text{ClPt}$ : 492.9; found: 498.1 ( $M\text{-Cl} + \text{MeCN}$ )<sup>+</sup> (100%) and ( $M\text{-Cl}$ )<sup>+</sup> (25%).

**F) Synthesis of the Ph-Pt complex:** All of the final  $\text{Pt}^{\text{II}}$  complexes were synthesized by following the methods reported earlier, where the corresponding acetylides were prepared by deprotonation with 5% NaOMe solution in MeOH followed by the addition of cyclometallated  $\text{Pt}^{\text{II}}(\text{C}^{\wedge}\text{N}^{\wedge}\text{NNPr})\text{Cl}$  complex precursor.

In a 250 mL round-bottomed flask, phenyl acetylene (0.022 mL, 0.2 mmol) was added under an argon atmosphere. Anhydrous methanol (30 mL) was added to this. NaOMe (0.5 M, 3 mL) was added to this solution and stirred for 3 h at room temperature under inert atmosphere.  $\text{Pt}^{\text{II}}(\text{C}^{\wedge}\text{N}^{\wedge}\text{N})\text{Cl}$  complex (0.1182 g, 0.24 mmol) dissolved in  $\text{CHCl}_3$  (20 mL) was added to the phenyl acetylide solution and the solution was stirred for 1 day at 60 °C in the dark. After removing the solvent under reduced pressure and aqueous extraction with 250 mL DCM, the crude mixture was purified by column chromatography on  $\text{SiO}_2$  using dichloromethane as eluent.

**Ph-Pt:** Yield ca. 45%;  $^1\text{H}$  NMR (500 MHz,  $\text{CDCl}_3$ , 298 K, TMS):  $\delta$  = 0.89 (t,  $J$  = 7.3 Hz, 3H), 1.99 (sextet,  $J$  = 7.3 Hz, 2H), 4.59 (t,  $J$  = 7.2 Hz, 2H), 6.54 (d,  $J$  = 2.6 Hz, 1H), 6.99 (td,  $J$  = 7.4 Hz,  $J$  = 1.2 Hz, 1H), 7.09–7.15 (m, 2H), 7.18 (dd,  $J$  = 7.7 Hz,  $J$  = 0.7 Hz, 1H), 7.23–7.29 (m, 3H), 7.33 (d,  $J$  = 8.1 Hz, 1H), 7.40 (d,  $J$  = 2.6 Hz, 1H), 7.46 (dd,  $J$  = 8.2 Hz,  $J$  = 1.2 Hz, 2H), 7.60 (t,  $J$  = 7.9 Hz, 1H), 8.04 ppm (dd,  $J$  = 7.6 Hz,  $J$  = 0.8 Hz, 1H);  $^{13}\text{C}$  NMR spectra (125 MHz,  $\text{CDCl}_3$ , 298 K, TMS):  $\delta$  = 10.9, 24.3, 54.4, 105.0, 115.8, 116.3, 124.0, 124.1, 130.7, 132.4, 133.9, 138.4, 138.8, 145.8, 150.7, 152.6, 166.5 ppm; ESI-MS:  $m/z$  calcd for  $\text{C}_{25}\text{H}_{21}\text{N}_3\text{Pt}$ : 558.5; found: 559.1 ( $M + \text{H}$ )<sup>+</sup> (100%) and 279.2 ( $M$ )<sup>2+</sup> (45%).

**G) Synthesis of the porphyrin-Pt<sup>II</sup> conjugate, P-Pt1:** In a 250 mL round-bottomed flask, **1P** (0.0419 g, 0.025 mmol) was added. This was evacuated and back-filled with argon several times. Anhydrous methanol (10 mL) was added to this. NaOMe (0.5 M, 1 mL) was added to this and stirred for 3 h at room temperature under inert atmosphere.  $\text{Pt}^{\text{II}}(\text{C}^{\wedge}\text{N}^{\wedge}\text{N})\text{Cl}$  (0.0148 g, 0.03 mmol) dissolved in  $\text{CHCl}_3$  (20 mL) and MeOH (10 mL) was added to the porphyrin acetylide solution and the solution was stirred for 1 day at 60 °C in dark. After removing the solvent under reduced pressure and aqueous extraction with DCM (150 mL) the crude mixture was purified by column chromatography on  $\text{SiO}_2$  using dichloromethane-methanol (95:5 v/v) as eluent. A second chromatography using silica gel is necessary for further purification.

**P-Pt1:** Yield ca. 60%;  $^1\text{H}$  NMR (500 MHz,  $\text{CDCl}_3$ , 298 K, TMS):  $\delta$  = 1.12 (t,  $J$  = 7.3 Hz, 3H), 2.23 (sextet,  $J$  = 7.3 Hz, 2H), 2.94–2.96 (m, 18H),

3.11–3.15 (m, 12H), 3.29–3.34 (m, 12H), 3.53–3.57 (m, 12H), 3.66–3.69 (m, 12H), 3.86–3.89 (m, 12H), 4.26–4.29 (m, 12H), 4.84 (t,  $J = 7.3$  Hz, 2H), 6.64 (d,  $J = 2.5$  Hz, 1H), 6.89–6.92 (m, 3H), 7.09 (td,  $J = 7.4$  Hz,  $J = 1.0$  Hz, 1H), 7.26–7.29 (m, 2H), 7.36 (dd,  $J = 7.7$  Hz,  $J = 1.1$  Hz, 1H), 7.41 (s, 1H), 7.43–7.44 (m, 6H), 7.54 (d,  $J = 2.5$  Hz, 1H), 7.68 (t,  $J = 8.0$  Hz, 1H), 7.86 (d,  $J = 8.0$  Hz, 2H), 8.09 (d,  $J = 8.0$  Hz, 2H), 8.28 (dd,  $J = 7.6$  Hz,  $J = 1.0$  Hz, 1H), 8.96–8.98 (m, 4H), 8.99 (d,  $J = 4.6$  Hz, 2H), 9.02 ppm (d,  $J = 4.6$  Hz, 2H);  $^{13}\text{C}$  NMR spectra (125 MHz,  $\text{CDCl}_3$ , 298 K, TMS):  $\delta = 11.2, 24.6, 55.6, 58.6, 67.9, 69.9, 70.2, 70.5, 70.6, 70.8, 71.5, 101.4, 102.4, 105.3, 106.9, 114.7, 115.6, 116.4, 120.3, 120.5, 121.6, 123.7, 124.4, 128.0, 129.8, 131.3, 131.8, 132.0, 134.3, 137.9, 139.3, 139.4, 139.6, 144.9, 146.3, 149.8, 150.2, 150.7, 154.3, 157.8, 165.4$  ppm; MALDI-TOF-MS:  $m/z$  calcd for  $\text{C}_{105}\text{H}_{127}\text{N}_7\text{O}_{24}\text{ZnPt}$ : 2131.6; found: 2131.1 (100%).

**Synthesis of the porphyrin–Pt<sup>II</sup> conjugate, P-Pt2:** In a 250 mL round-bottomed flask, bis(phenylacetylene)porphyrin (0.1031 g, 0.075 mmol) was added. This was evacuated and back-filled with argon several times. Anhydrous methanol (30 mL) was added to this. Then NaOMe (0.5 mL, 3 mL) was added to the reaction mixture and stirred for 3 h at room temperature under an inert atmosphere. Thereafter Pt<sup>II</sup>C<sup>^</sup>NNNPr (0.111 g, 0.225 mmol) dissolved in  $\text{CHCl}_3$  (30 mL) and MeOH (20 mL) was added to the porphyrin acetylide solution and the solution was stirred for 2 days at 60 °C in dark. After removing the solvent under reduced pressure and aqueous extraction with DCM (250 mL), the crude mixture was purified by column chromatography on  $\text{SiO}_2$  using DCM–MeOH mixture (97:4 v/v) as eluent. A second purification by silica gel chromatography may be necessary.

**P-Pt2:** Yield ca. 58%;  $^1\text{H}$  NMR (500 MHz,  $\text{CDCl}_3$ , 298 K, TMS):  $\delta = 1.11$  (t,  $J = 7.3$  Hz, 6H), 2.21 (sextet,  $J = 7.3$  Hz, 4H), 2.85 (s, 12H), 2.99–3.02 (m, 8H), 3.19–3.21 (m, 8H), 3.44–3.46 (m, 8H), 3.59–3.61 (m, 8H), 3.80–3.82 (m, 8H), 4.23–4.25 (m, 8H), 4.82 (t,  $J = 7.3$  Hz, 4H), 6.59 (d,  $J = 2.5$  Hz, 2H), 6.87 (t,  $J = 2.2$  Hz, 2H), 7.07 (td,  $J = 7.4$  Hz,  $J = 1.1$  Hz, 2H), 7.21–7.27 (m, 4H), 7.33 (dd,  $J = 7.8$  Hz,  $J = 1.0$  Hz, 2H), 7.36 (dd,  $J = 7.7$  Hz,  $J = 1.0$  Hz, 2H), 7.44 (d,  $J = 2.2$  Hz, 4H), 7.50 (d,  $J = 2.4$  Hz, 2H), 7.62 (t,  $J = 7.9$  Hz, 2H), 7.86 (d,  $J = 8.1$  Hz, 4H), 8.12 (d,  $J = 8.1$  Hz, 4H), 8.26 (dd,  $J = 7.6$  Hz,  $J = 1.0$  Hz, 2H), 9.00 (d,  $J = 4.6$  Hz, 4H), 9.03 ppm (d,  $J = 4.6$  Hz, 4H);  $^{13}\text{C}$  NMR spectra (125 MHz,  $\text{CDCl}_3$ , 298 K, TMS):  $\delta = 11.2, 24.6, 55.5, 58.6, 67.9, 69.9, 70.1, 70.5, 70.7, 71.4, 101.4, 102.6, 105.3, 106.8, 114.8, 115.6, 116.3, 120.5, 121.3, 123.7, 124.4, 128.1, 129.8, 131.2, 131.5, 131.8, 132.2, 134.4, 137.9, 139.2, 139.6, 144.9, 146.3, 149.7, 149.9, 150.3, 150.6, 154.2, 157.8, 165.3$  ppm; MALDI-TOF-MS:  $m/z$  calcd for  $\text{C}_{110}\text{H}_{114}\text{N}_{10}\text{O}_{16}\text{ZnPt}_2$ : 2287.7; found: 2287.1 (100%).

**Synthesis of the porphyrin–Pt<sup>II</sup> conjugate, P-Pt3:** By following the same synthetic route applied before, P-Pt3 was prepared. Typically this was carried out by taking 3P (0.10745 g, 0.1 mmol) in a 250 mL three-necked round-bottomed flask. This was evacuated and back-filled by argon several times. Anhydrous  $\text{CHCl}_3$  (30 mL) and methanol (20 mL) was added to it and stirred vigorously to dissolve the solid mass completely. Then NaOMe (0.5 mL, 10 mL) was added and stirred for 4 h at room temperature under an inert atmosphere. Finally, Pt<sup>II</sup>(C<sup>^</sup>NN)Cl complex (0.2464 g, 0.5 mmol) dissolved in  $\text{CHCl}_3$  (30 mL) and methanol (20 mL) was added to the porphyrin acetylide solution and the stirred for 2 days at 60 °C in the dark. After removing the solvent under reduced pressure and aqueous extraction with DCM (500 mL), the crude mixture was purified by column chromatography on  $\text{Al}_2\text{O}_3$  (Brockmann III) using a dichloromethane–methanol mixture (99:1 v/v) as eluent.

**P-Pt3:** Yield ca. 50%;  $^1\text{H}$  NMR (500 MHz,  $\text{CDCl}_3$ , 298 K, TMS):  $\delta = 1.06$  (t,  $J = 7.3$  Hz, 9H), 2.14 (sextet,  $J = 7.3$  Hz, 6H), 3.11 (s, 6H), 3.28–3.30 (m, 4H), 3.42–3.44 (m, 4H), 3.54–3.56 (m, 4H), 3.64–3.66 (m, 4H), 3.84–3.86 (m, 4H), 4.23–4.25 (m, 4H), 4.71–4.77 (m, 6H),

6.44 (d,  $J = 2.5$  Hz, 1H), 6.51 (d,  $J = 2.5$  Hz, 2H), 6.87 (t,  $J = 2.2$  Hz, 1H), 6.99–7.05 (m, 3H), 7.10 (d,  $J = 7.7$  Hz, 1H), 7.16 (d,  $J = 7.7$  Hz, 2H), 7.18–7.25 (m, 4H), 7.27–7.33 (m, 5H), 7.38 (d,  $J = 2.5$  Hz, 1H), 7.40 (d,  $J = 2.2$  Hz, 2H), 7.44 (d,  $J = 2.5$  Hz, 2H), 7.51 (t,  $J = 8.0$  Hz, 1H), 7.57 (t,  $J = 8.0$  Hz, 2H), 7.82 (dd,  $J = 8.0$  Hz,  $J = 1.3$  Hz, 6H), 8.09 (dd,  $J = 8.0$  Hz,  $J = 1.3$  Hz, 6H), 8.22 (td,  $J = 7.7$  Hz,  $J = 1.0$  Hz, 3H), 8.93–8.99 ppm (m, 8H);  $^{13}\text{C}$  NMR spectra (125 MHz,  $\text{CDCl}_3$ , 298 K, TMS):  $\delta = 11.0, 24.4, 55.4, 58.7, 67.7, 69.7, 70.2, 70.4, 70.6, 71.5, 101.0, 102.2, 105.2, 106.8, 114.7, 115.6, 116.2, 119.8, 120.8, 123.6, 124.3, 127.6, 129.5, 131.1, 131.4, 131.8, 134.4, 137.7, 139.2, 139.9, 145.2, 146.3, 149.6, 149.9, 150.0, 150.5, 154.1, 157.6, 165.0$  ppm; MALDI-TOF-MS:  $m/z$  calcd for  $\text{C}_{115}\text{H}_{101}\text{N}_{13}\text{O}_8\text{ZnPt}_3$ : 2443.7; found: 2443.6 (100%).

## Acknowledgements

We thank the European Commission for a Marie-Curie fellowship to A.J. The authors declare no competing financial interest.

**Keywords:** acetylide complexes · energy transfer · platinum · porphyrins · singlet oxygen · zinc

- [1] a) N. Aratani, H. S. Cho, T. K. Ahn, S. Cho, D. Kim, H. Sumi, A. Osuka, *J. Am. Chem. Soc.* **2003**, *125*, 9668–9681; b) Y. Nakamura, I.-W. Hwang, N. Aratani, T. K. Ahn, D. M. Ko, A. Takagi, T. Kawai, T. Matsumoto, D. Kim, A. Osuka, *J. Am. Chem. Soc.* **2005**, *127*, 236–246; c) R. P. Briñas, T. Troxler, R. M. Hochstrasser, S. A. Vinogradov, *J. Am. Chem. Soc.* **2005**, *127*, 11851–11862; d) C. Huo, H. Zhang, H. Zhang, H. Zhang, B. Yang, P. Zhang, Y. Wang, *Inorg. Chem.* **2006**, *45*, 4735–4742; e) F. Hajjaj, Z. S. Yoon, M.-C. Yoon, J. Park, A. Satake, D. Kim, Y. Kobuke, *J. Am. Chem. Soc.* **2006**, *128*, 4612–4623; f) J. B. Oh, M.-K. Nah, Y. H. Kim, M. S. Kang, J.-W. Ka, H. K. Kim, *Adv. Funct. Mater.* **2007**, *17*, 413–424; g) I. Hisaki, S. Hiroto, K. S. Kim, S. B. Noh, D. Kim, H. Shinokubo, A. Osuka, *Angew. Chem. Int. Ed.* **2007**, *46*, 5125–5128; *Angew. Chem.* **2007**, *119*, 5217–5220; h) T. Hori, X. Peng, N. Aratani, A. Takagi, T. Matsumoto, T. Kawai, Z. S. Yoon, M.-C. Yoon, J. Yang, D. Kim, A. Osuka, *Chem. Eur. J.* **2008**, *14*, 582–595; i) O. S. Finikova, P. Chen, K. M. Kadish, S. A. Vinogradov, *J. Photochem. Photobiol. A* **2008**, *198*, 75–84; j) A. Jana, M. Ishida, K. Kwak, Y. M. Sung, D. S. Kim, V. M. Lynch, D. Lee, D. Kim, J. L. Sessler, *Chem. Eur. J.* **2013**, *19*, 338–349.
- [2] a) T. B. Norsten, N. R. Branda, *Adv. Mater.* **2001**, *13*, 347–349; b) G. S. He, L.-S. Tan, Q. Zheng, P. N. Prasad, *Chem. Rev.* **2008**, *108*, 1245–1330; c) M. Pawlicki, H. A. Collins, R. G. Denning, H. L. Anderson, *Angew. Chem. Int. Ed.* **2009**, *48*, 3244–3266; *Angew. Chem.* **2009**, *121*, 3292–3316.
- [3] a) W. M. Campbell, A. K. Burrell, D. L. Officer, K. W. Jolley, *Coord. Chem. Rev.* **2004**, *248*, 1363–1379; b) A. J. Mozer, M. J. Griffith, G. Tsekouras, P. Wagner, G. G. Wallace, S. Mori, K. Sunahara, M. Miyashita, J. C. Earles, K. C. Gordon, L. Du, R. Katoh, A. Furube, D. L. Officer, *J. Am. Chem. Soc.* **2009**, *131*, 15621–15623; c) K. Kurotobi, Y. Toude, K. Kawamoto, Y. Fujimori, S. Ito, P. Chabera, V. Sundström, H. Imahori, *Chem. Eur. J.* **2013**, *19*, 17075–17081; d) E. W.-G. Diao, L.-L. Li, Eds. K. M. Kadish, K. M. Smith, R. Guilard, *Handb. Porphyrin Sci.* **2014**, *28*, 279–317; e) J. Luo, M. Xu, R. Li, K.-W. Huang, C. Jiang, Q. Qi, W. Zeng, J. Zhang, C. Chi, P. Wang, J. Wu, *J. Am. Chem. Soc.* **2014**, *136*, 265–272; f) Y. Wang, B. Chen, W. Wu, X. Li, W. Zhu, H. Tian, Y. Xie, *Angew. Chem. Int. Ed.* **2014**, *53*, 10779–10783; *Angew. Chem.* **2014**, *126*, 10955–10959; g) T. Zhang, X. Qian, P.-F. Zhang, Y.-Z. Zhu, J.-Y. Zheng, *Chem. Commun.* **2015**, *51*, 3782–3785; h) Z. E. Galateia, N. Agapi, N. Vasilis, G. D. Sharma, C. G. Athanassios, *J. Mater. Chem. C* **2015**, *3*, 5652–5664.
- [4] a) R. Bonnett, *Chem. Soc. Rev.* **1995**, *24*, 19–33; b) J. L. Sessler, R. A. Miller, *Biochem. Pharmacol.* **2000**, *59*, 733–739; c) J. Seenisamy, S. B. Shyam, V. Gokhale, H. Vankayalapati, D. Sun, A. Siddiqui-Jain, N. Streiner, K. Shin-ya, E. White, W. D. Wilson, L. H. Hurley, *J. Am. Chem. Soc.* **2005**, *127*, 2944–2959; d) H. Mukai, Y. Wada, Y. Watanabe, *Ann. Nucl. Med.* **2013**, *27*, 625–639; e) A. Naik, R. Rubbiani, G. Gasser, B. Spingler,

- Angew. Chem. Int. Ed.* **2014**, *53*, 6938–6941; *Angew. Chem.* **2014**, *126*, 7058–7061; f) J. Lu, W. Zhang, L. Yuan, W. Ma, X. Li, W. Lu, Y. Zhao, G. Chen, *Macromol. Biosci.* **2014**, *14*, 340–346; g) J. Schmitt, V. Heitz, A. Sour, F. Bolze, H. Ftouni, J.-F. Nicoud, L. Flamigni, B. Ventura, *Angew. Chem. Int. Ed.* **2015**, *54*, 169–173; *Angew. Chem.* **2015**, *127*, 171–175.
- [5] a) S. Mathai, D. K. Bird, S. S. Stylli, T. A. Smith, K. P. Ghiggino, *Photochem. Photobiol. Sci.* **2007**, *6*, 1019–1026; b) T. Zhao, H. Wu, S. Q. Yao, Q.-H. Xu, G. Q. Xu, *Langmuir* **2010**, *26*, 14937–14942; c) M. Nowostawska, S. A. Corr, S. J. Byrne, J. Conroy, Y. Volkov, Y. K. Guńko, *J. Nanobiotechnol.* **2011**, *9*, 13.
- [6] a) M. C. DeRosa, R. J. Crutchley, *Coord. Chem. Rev.* **2002**, *233–234*, 351–371; b) D. E. J. G. Dolmans, D. Fukumura, R. K. Jain, *Nature* **2003**, 380–387; c) J. F. Lovell, T. W. B. Liu, J. Chen, G. Zheng, *Chem. Rev.* **2010**, *110*, 2839–2857; d) E. Secret, M. Maynadier, A. Gallud, A. Chaix, E. Bouffard, M. Gary-Bobo, N. Marcotte, O. Mongin, K. E. Cheikh, V. Hugues, M. Auffan, C. Frochot, A. Morère, P. Maillard, M. Blanchard-Desce, M. J. Sailor, M. Garcia, J.-O. Durand, F. Cunin, *Adv. Mater.* **2014**, *26*, 7643–7648; e) L. Xu, L. Liu, F. Liu, W. Li, R. Chen, Y. Gao, W. Zhang, *J. Mater. Chem. B* **2015**, *3*, 3062–3071; f) J. Park, D. Feng, S. Yuan, H.-C. Zhou, *Angew. Chem. Int. Ed.* **2015**, *54*, 430–435; *Angew. Chem.* **2015**, *127*, 440–445.
- [7] a) A. Mazzaglia, A. Valerio, N. Micali, V. Villari, F. Quaglia, M. A. Castriciana, L. M. Sclaro, M. Giuffrè, G. Siracusano, M. T. Sciortino, *Chem. Commun.* **2011**, *47*, 9140–9142; b) K. Hayashi, M. Nakamura, K. Ishimura, *Chem. Commun.* **2012**, *48*, 3830–3832; c) M. Novaira, M. P. Cormick, E. N. Durantini, *J. Photochem. Photobiol. A* **2012**, *246*, 67–74; d) T. Zhang, C.-F. Chan, R. Lan, H. Li, N.-K. Mak, W.-K. Wong, K.-L. Wong, *Chem. Commun.* **2013**, *49*, 7252–7254; e) L. Wang, H. Li, G. Fang, J. Zhou, D. Cao, *Sensors and Actuators B* **2014**, *196*, 653–662.
- [8] a) D. T. Gryko, C. Clausen, J. S. Lindsey, *J. Org. Chem.* **1999**, *64*, 8635–8647; b) R. L. Carroll, C. B. Gorman, *Angew. Chem. Int. Ed.* **2002**, *41*, 4378–4400; *Angew. Chem.* **2002**, *114*, 4556–4579 and references therein; c) H. Imahori, S. Fukuzumi, *Adv. Funct. Mater.* **2004**, *14*, 525–536; d) D. A. Jose, A. D. Shukla, G. Ramakrishna, D. K. Palit, H. N. Ghosh, A. Das, *J. Phys. Chem. B* **2007**, *111*, 9078–9087; e) M. Jurow, A. E. Schuckman, J. D. Batteas, C. M. Drain, *Coord. Chem. Rev.* **2010**, *254*, 2297–2310; f) S. Mohnani, D. Bonifazi, *Coord. Chem. Rev.* **2010**, *254*, 2342–2362; g) M. J. Latter, S. J. Langford, *Int. J. Mol. Sci.* **2010**, *11*, 1878–1887; h) *Multiporphyrin Arrays: Fundamentals and Applications*, (Ed.: D. Kim), Pan Stanford Publishing, Singapore, **2012**; i) M. J. Griffith, K. Sunahara, P. Wagner, K. Wagner, G. G. Wallace, D. L. Officer, A. Furube, R. Katoh, S. Mori, A. J. Mozer, *Chem. Commun.* **2012**, *48*, 4145–4162; j) J. Rawson, A. C. Stuart, W. You, M. J. Therien, *J. Am. Chem. Soc.* **2014**, *136*, 17561–17569; k) T. Tanaka, A. Osuka, *Chem. Soc. Rev.* **2015**, *44*, 943–969.
- [9] a) V. W. W. Yam, K. M. C. Wong, N. Zhu, *J. Am. Chem. Soc.* **2002**, *124*, 6506–6507; b) V. W. W. Yam, K. H. Y. Chan, K. M. C. Wong, N. Zhu, *Chem. Eur. J.* **2005**, *11*, 4535–4543; c) H. S. Lo, S. K. Yip, K. M. C. Wong, N. Zhu, V. W. W. Yam, *Organometallics* **2006**, *25*, 3537–3540; d) C. Yu, K. H. Y. Chan, K. M. C. Wong, V. W. W. Yam, *Chem. Commun.* **2009**, 3756–3758; e) K. M. C. Wong, V. W. W. Yam, *Acc. Chem. Res.* **2011**, *44*, 424–434; f) C. Y.-S. Chung, V. W. W. Yam, *J. Am. Chem. Soc.* **2011**, *133*, 18775–18784; g) S. Y.-L. Leung, W. H. Lam, V. W. W. Yam, *Proc. Natl. Acad. Sci. USA* **2013**, *110*, 7986–7991; h) Y. Tanaka, K. M.-C. Wong, V. W. W. Yam, *Chem. Eur. J.* **2013**, *19*, 390–399; i) C. Y.-S. Chung, V. W. W. Yam, *Chem. Sci.* **2013**, *4*, 377–387.
- [10] a) S. J. Farley, D. L. Rochester, A. L. Thompson, J. A. K. Howard, J. A. G. Williams, *Inorg. Chem.* **2005**, *44*, 9690–9703; b) S. W. Botchway, M. Charnley, J. W. Haycock, A. W. Parker, D. L. Rochester, J. A. Weinstein, J. A. G. Williams, *Proc. Natl. Acad. Sci. USA* **2008**, *105*, 16071–16076; c) E. Rossi, A. Colombo, C. Dragonetti, D. Roberto, R. Ugo, A. Valore, L. Falcioia, P. Brulatti, M. Cocchi, J. A. G. Williams, *J. Mater. Chem.* **2012**, *22*, 10650–10655; d) E. S.-H. Lam, D. P.-K. Tsang, W. H. Lam, A. Y.-Y. Tam, M.-Y. Chan, W.-T. Wong, V. W. W. Yam, *Chem. Eur. J.* **2013**, *19*, 6385–6397.
- [11] S. Y.-L. Leung, E. S.-H. Lam, W. H. Lam, K. M.-C. Wong, W.-T. Wong, V. W. W. Yam, *Chem. Eur. J.* **2013**, *19*, 10360–10369.
- [12] a) W. Lu, B.-X. Mi, M. C. W. Chan, Z. Hui, N. Zhu, S.-T. Lee, C.-M. Che, *Chem. Commun.* **2002**, 206–207; b) W. Lu, B.-X. Mi, M. C. W. Chan, Z. Hui, C.-M. Che, N. Zhu, S.-T. Lee, *J. Am. Chem. Soc.* **2004**, *126*, 4958–4971; c) C.-K. Koo, Y.-M. Ho, C.-F. Chow, M. H.-W. Lam, T.-C. Lau, W.-Y. Wong, *Inorg. Chem.* **2007**, *46*, 3603–3612; d) C.-K. Koo, K.-L. Wong, C. W.-Y. Man, Y.-W. Lam, L. K.-Y. So, H.-L. Tam, S.-W. Tsao, K.-W. Cheah, K.-C. Lau, Y.-Y. Yang, J.-C. Chen, M. H.-W. Lam, *Inorg. Chem.* **2009**, *48*, 872–878; e) C.-K. Koo, L. K.-Y. So, K.-L. Wong, Y.-M. Ho, Y.-W. Lam, M. H.-W. Lam, K.-W. Cheah, C. C.-W. Cheng, W.-M. Kwok, *Chem. Eur. J.* **2010**, *16*, 3942–3950.
- [13] a) C. Monnereau, J. Gomez, E. Blart, F. Odobel, S. Wallin, A. Fallberg, L. Hammarström, *Inorg. Chem.* **2005**, *44*, 4806–4817; b) E. Göransson, J. Boixel, C. Monnereau, E. Blart, Y. Pellegrin, H.-C. Becker, L. Hammarström, F. Odobel, *Inorg. Chem.* **2010**, *49*, 9823–9832.
- [14] a) R. C. Jagessar, J. M. Tour, *Org. Lett.* **2000**, *2*, 111–113; b) K. Susumu, M. J. Therien, *J. Am. Chem. Soc.* **2002**, *124*, 8550–8552; c) S. Drouet, A. Merhi, D. Yao, M. P. Cifuentes, M. G. Humphrey, M. Wielgus, J. Olesiak-Banska, K. Matczyszyn, M. Samoc, F. Paul, C. O. Paul-Roth, *Tetrahedron* **2012**, *68*, 10351–10359.
- [15] a) E. E. Jelley, *Nature* **1936**, *138*, 1009–1010; b) G. Scheibe, *Angew. Chem.* **1937**, *50*, 212; c) K.-P. S. Dancil, L. F. Hilario, R. G. Khoury, K. U. Mai, C. K. Nguyen, K. S. Weddle, A. M. Shachter, *J. Heterocycl. Chem.* **1997**, *34*, 749–755; d) H. Imahori, H. Norieda, Y. Nishimura, I. Yamazaki, K. Higuchi, N. Kato, T. Motohiro, H. Yamada, K. Tamaki, M. Arimura, Y. Sakata, *J. Phys. Chem. B* **2000**, *104*, 1253–1260; e) K. Zelenka, T. Trnka, I. Tišlerová, D. Monti, S. Cinti, M. L. Naitana, L. Schiaffino, M. Venanzi, G. Laguzzi, L. Luvidi, G. Mancini, Z. Nováková, O. Šimák, Z. Wimmer, P. Drašar, *Chem. Eur. J.* **2011**, *17*, 13743–13753; f) X.-D. Xu, J. Zhang, L.-J. Chen, R. Guo, D.-X. Wang, H.-B. Yang, *Chem. Commun.* **2012**, *48*, 11223–11225; g) A. Jana, H. Gobeze, M. Ishida, T. Mori, A. Ariga, J. P. Hill, F. D'Souza, *Dalton Trans.* **2015**, *44*, 359–367.
- [16] a) R. Schmidt, C. Tanielian, R. Dunsbach, C. Wolff, *J. Photochem. Photobiol. A* **1994**, *79*, 11–17; b) N. M. Shavaleev, H. Adams, J. Best, R. Edge, S. Navaratnam, J. A. Weinstein, *Inorg. Chem.* **2006**, *45*, 9410–9415.
- [17] Gaussian 09, Revision A.1, M. J. Frisch, G. W. Trucks, H. B. Schlegel, G. E. Scuseria, M. A. Robb, J. R. Cheeseman, G. Scalmani, V. Barone, B. Menonucci, G. A. Petersson, H. Nakatsuji, M. Caricato, X. Li, H. P. Hratchian, A. F. Izmaylov, J. Bloino, G. Zheng, J. L. Sonnenberg, M. Hada, M. Ehara, K. Toyota, R. Fukuda, J. Hasegawa, M. Ishida, T. Nakajima, Y. Honda, O. Kitao, H. Nakai, T. Vreven, J. A. Montgomery, Jr., J. E. Peralta, F. Ogliaro, M. Bearpark, J. J. Heyd, E. Brothers, K. N. Kudin, V. N. Staroverov, R. Kobayashi, J. Normand, K. Raghavachari, A. Rendell, J. C. Burant, S. S. Iyengar, J. Tomasi, M. Cossi, N. Rega, N. J. Millam, M. Klene, J. E. Knox, J. B. Cross, V. Bakken, C. Adamo, J. Jaramillo, R. Gomperts, R. E. Stratmann, O. Yazyev, A. J. Austin, R. Cammi, C. Pomelli, J. W. Ochterski, R. L. Martin, K. Morokuma, V. G. Zakrzewski, G. A. Voth, P. Salvador, J. J. Dannenberg, S. Dapprich, A. D. Daniels, Ö. Farkas, J. B. Foresman, J. V. Ortiz, J. Cioslowski, D. J. Fox, Gaussian, Inc., Wallingford CT, **2009**.
- [18] a) C. Lee, W. Yang, R. G. Parr, *Phys. Rev. B* **1988**, *37*, 785–789; b) A. D. Becke, *J. Chem. Phys.* **1993**, *98*, 5648–5652; c) O. Rubio-Pons, Y. Luo, H. Ågren, *J. Chem. Phys.* **2006**, *124*, 094310.
- [19] a) P. J. Hay, W. R. Wadt, *J. Chem. Phys.* **1985**, *82*, 270–283; b) W. R. Wadt, P. J. Hay, *J. Chem. Phys.* **1985**, *82*, 284–298; c) P. J. Hay, W. R. Wadt, *J. Chem. Phys.* **1985**, *82*, 299–310.
- [20] C. B. Nielsen, M. Johnsen, J. Arnbjerg, M. Pittelkow, S. P. McIlroy, P. R. Ogilby, M. Jørgensen, *J. Org. Chem.* **2005**, *70*, 7065–7079.
- [21] G. M. Sheldrick, SADABS: A Program for Absorption Correction with the Siemens SMART System; University of Göttingen: Germany, **1996**.
- [22] G. M. Sheldrick, *Acta Crystallogr. Sect. A* **2008**, *64*, 112–122.
- [23] WinGX 1.64: An Integrated System of Windows Programs for the Solution, Refinement and Analysis of Single Crystal X-ray Diffraction Data; L. J. Farrugia, *J. Appl. Crystallogr.* **1999**, *32*, 837–838.
- [24] *International Tables for X-ray Crystallography, Vol. C*, Tables 4.2.6.8 and 6.1.1.4 (Ed.: A. J. C. Wilson), Kluwer Academic Press, Boston, **1992**.
- [25] a) D. Lötscher, S. Rupprecht, H. Stoeckli-Evans, A. Zelewsky, *Tetrahedron: Asymmetry* **2000**, *11*, 4341–4357; b) C.-K. Koo, B. Lam, S.-K. Leung, M. H.-W. Lam, W.-Y. Wong, *J. Am. Chem. Soc.* **2006**, *128*, 16434–16435.

Received: November 10, 2015

Revised: December 23, 2015

Published online on February 5, 2016